
Strong electronic correlations in superconducting organic charge transfer salts.

B. J. Powell and Ross H. McKenzie

Department of Physics, University of Queensland, Brisbane, Queensland 4072, Australia. powell@physics.uq.edu.au

Summary. We review the role of strong electronic correlations in quasi-two-dimensional organic charge transfer salts such as $(\text{BEDT-TTF})_2X$, $(\text{BETS})_2Y$ and β' - $[\text{Pd}(\text{dmit})_2]_2Z$. We begin by defining minimal models for these materials. It is necessary to identify two classes of material: the first class is strongly dimerised and is described by a half-filled Hubbard model; the second class is not strongly dimerised and is described by a quarter filled extended Hubbard model. We argue that these models capture the essential physics of these materials. We explore the phase diagram of the half-filled quasi-two-dimensional organic charge transfer salts, focusing on the metallic and superconducting phases. We review work showing that the metallic phase, which has both Fermi liquid and ‘bad metal’ regimes, is described both quantitatively and qualitatively by dynamical mean field theory (DMFT). The phenomenology of the superconducting state is still a matter of contention. We critically review the experimental situation, focusing on the key experimental results that may distinguish between rival theories of superconductivity, particularly probes of the pairing symmetry and measurements of the superfluid stiffness. We then discuss some strongly correlated theories of superconductivity, in particular, the resonating valence bond (RVB) theory of superconductivity. We conclude by discussing some of the major challenges currently facing the field. These include: parameterising minimal models; the evidence for a pseudogap from nuclear magnetic resonance (NMR) experiments; superconductors with low critical temperatures and extremely small superfluid stiffnesses; the possible spin-liquid states in κ -(ET) $_2\text{Cu}_2(\text{CN})_3$ and β' - $[\text{Pd}(\text{dmit})_2]_2Z$; and the need for high quality large single crystals.

1.1 Motivation and scope

The Drude, Sommerfeld and Bloch models explain many of the properties of elemental metals and alloys in terms of a theory of non-interacting electrons. This is somewhat surprising as for typical metals the radius of a sphere whose volume is equal to the volume per conduction electron is of order 1 \AA [1]. Thus, one naïvely expects that the Coulomb interaction between electrons will be large. Therefore, one of the most significant achievements in condensed matter theory is Landau’s theory of Fermi liquids [2] which explains, through the idea

of adiabatic continuity, why the Coulomb interaction simply renormalises the weakly interacting electron gas.

However, in many “strongly correlated” systems interactions qualitatively alter the behaviour of the material. For example, in the Kondo effect the interactions between the conduction electrons and magnetic impurities, which leads to a logarithmic increase in the resistivity at low temperatures, cannot be described by perturbation theory from the Fermi liquid state [3]. Indeed even the BCS state [4] is not adiabatically connected to the Fermi liquid ground state. The Kondo effect is now well understood, but many other strongly correlated phases are not, e.g., high temperature superconductivity and the pseudogap in the cuprates [5], colossal magnetoresistance in the manganites [6] and emergence of unconventional superconductivity in heavy fermion materials [7].

The non-perturbative nature of strongly correlated materials presents several major challenges to theory. For example some big questions are: What is the appropriate description of the metallic state when the system is near to an instability to a Mott insulating state? What are the connections between magnetic ordering and unconventional superconductivity? Under what conditions can an antiferromagnet have a spin-liquid ground state and/or spinon excitations? When superconductivity is found near a Mott transition, what is the relationship between the symmetry of the superconducting state and the ground state of the parent Mott insulator? What is the appropriate microscopic description of a metallic state with a pseudogap? What are the mechanisms responsible for unconventional superconductivity and what are the appropriate microscopic descriptions of such states? Many of these questions are deeply intertwined.

Organic charge transfer salts are excellent model systems in which to study many of the questions about the strongly correlated phenomena described above. Band structure suggests that these materials should be metals at all experimentally relevant pressures and temperatures. However, as we will discuss below, the observed phases include, Mott insulators, Néel antiferromagnets, spin-liquids, (unconventional) superconductors, Fermi liquids, a pseudogap and a ‘bad metal’. Further, organic chemistry allows the organic charge transfer salts to be subtly tuned in ways that have never been achieved in inorganic materials. A rather beautiful example of this is that in κ -(ET)₂Cu[N(CN)₂]Br the Mott transition can be driven by replacing the eight hydrogen atoms in the ET molecule with deuterium [8]. Indeed the chemistry can be controlled to such an extent that the number of H/D atoms on each ET molecule can be varied uniformly throughout the entire sample allowing one to move gradually across the Mott transition and observe the coexistence of the insulating and superconducting phases expected because the transition is first order [9].

We will argue below that, despite the chemical complexity of the organic charge transfer salts, the physics boils down to that of the Hubbard model on various lattices and at either half or one quarter filling. We will show

that the strongly correlated physics of the various polymorphs and chemical constituents can be described within this framework.

The Hamiltonian of the one-band Hubbard model is

$$\hat{\mathcal{H}}_{\text{Hubbard}} = - \sum_{ij,\sigma} (t_{ij} + \mu\delta_{ij}) \hat{c}_{i\sigma}^\dagger \hat{c}_{j\sigma} + U \sum_i \hat{n}_{i\uparrow} \hat{n}_{i\downarrow}, \quad (1.1)$$

where, t_{ij} is the hopping integral from the site i to the site j , μ is the chemical potential, U is the Coulomb repulsion caused by putting two electrons on the same site, $\hat{c}_{i\sigma}^{(\dagger)}$ annihilates (creates) an electron on site i with spin σ and the number operator $\hat{n}_{i\sigma} = \hat{c}_{i\sigma}^\dagger \hat{c}_{i\sigma}$. The Hubbard model is, perhaps, the simplest model that can describe strongly correlated physics and is therefore an important starting point for a complete and general description of strong correlations. Further, the Hubbard model is also believed to describe the essential physics of, for example, the cuprates [10] and the cobaltates [11].

At some points later in this review we will also wish to discuss extended Hubbard models. In particular we will discuss the Coulomb repulsion when two electrons are placed on neighbouring sites, we will refer to these as ‘ V ’ terms and the additional term in the Hamiltonian will be

$$\hat{\mathcal{H}}_V = V \sum_{\langle ij \rangle} (\hat{n}_{i\uparrow} + \hat{n}_{i\downarrow})(\hat{n}_{j\uparrow} + \hat{n}_{j\downarrow}), \quad (1.2)$$

where the angled brackets indicate the sum is over some specified set of neighbouring sites, e.g., nearest neighbours only. Another important term we may wish to include is the Heisenberg exchange or ‘ J ’ term

$$\hat{\mathcal{H}}_J = J \sum_{\langle ij \rangle} \hat{\mathbf{S}}_i \cdot \hat{\mathbf{S}}_j, \quad (1.3)$$

where the spin operator is $\hat{\mathbf{S}}_i = \sum_{\alpha\beta} \hat{c}_{i\alpha}^\dagger \boldsymbol{\sigma}_{\alpha\beta} \hat{c}_{i\beta}$ and $\boldsymbol{\sigma} = (\sigma_x, \sigma_y, \sigma_z)$ is the vector of Pauli matrices. Lastly we may wish to include phonons and the electron-phonon interaction in the model. The simplest approach is to include the ‘Holstein’ terms which treat dissipationless phononic modes via the terms

$$\hat{\mathcal{H}}_{\text{Holstein}} = \sum_{i\sigma\nu} g_\nu \left(\hat{a}_{i\nu}^\dagger + \hat{a}_{i\nu} \right) \hat{n}_{i\sigma} + \sum_{i\nu} \omega_\nu \hat{a}_{i\nu}^\dagger \hat{a}_{i\nu}, \quad (1.4)$$

where the $\hat{a}_{i\nu}^{(\dagger)}$ operators annihilate (create) a phonon in the ν^{th} mode on the i^{th} lattice site, ω_ν is the characteristic frequency of ν^{th} mode and g_ν is the electron-phonon coupling between an electron on site i and a phonon in the ν^{th} mode on site i .

This review is *not* intended to be comprehensive. Rather, we present our views of the physics relevant to understand these materials. This is not to say that we are the originators of all of these ideas, but rather to stress that, as with any healthy research field, there are a number of prominent researchers

who might disagree with the views expressed here. Space constraints will not permit us to discuss rival theories and interpretations of data at length, we therefore refer interested readers to some alternative points of view [12–14] and some more comprehensive reviews [15].

1.2 Minimal models

In this review we will mostly consider materials with chemical formulae of the form D_2X where D is an organic donor molecule, for example bis(ethylenedithio)tetrathiafulvalene [$C_{10}S_8H_8$] (often abbreviated as BEDT-TTF or ET) or bis(ethylenedithio)tetraselenafulvalene [$C_{10}Se_8H_8$] (BETS), and X is an anion, e.g., I_3 or $Cu[N(CN)_2]Br$. The anion accepts one electron from a pair of donor molecules which leads, at the level of band theory, to an insulating anionic layer and a metallic donor layer. The chemical complexity of the organic charge transfer salts mean that few first principles calculations have been reported [16–20]. However, these suggest that a tight-binding or Huckel description of the band structure is a reasonable approximation. In this tight binding description a molecule serves as a ‘site’ [21].

1.2.1 Quarter filled charge transfer salts - the β'' and θ phases

It is clear that in the model proposed by Kino and Fukuyama [21] (described above) one expects that there should be, on average, half a hole per site. This is indeed the case for the β'' and θ polymorphs. These show a subtle competition between metallic, charge ordered insulating and superconducting phases [22, 23]. It has been argued that this arises due to the competition of spin and charge fluctuations. These effects have been studied in the extended Hubbard (t - J' - V - U)¹ model on a square lattice [22, 23]. The importance, for the superconducting state, of the fact that the actual lattice has a rather lower symmetry than the square lattice has also been stressed recently [24].

1.2.2 Half-filled charge transfer salts - the β , β' , κ and λ phases

In the β , β' , κ and λ polymorphs there is a single intermolecular hopping integral that is significantly larger than the others. This led Kino and Fukuyama [21] to propose that these two molecules behave as a single site as the hopping between them is rapid enough that it can be integrated out of the effective low energy theory. The two molecules are often referred to as a ‘dimer’. However, it is important to note that this does not imply that the molecules are covalently bonded in the conventional use of the word; i.e., there are no C-C,

¹The J' indicates that the exchange term is to next nearest neighbours. The J term can be neglected because in (or near) the charge ordered phase there are no (few) occupied sites with occupied nearest neighbours.

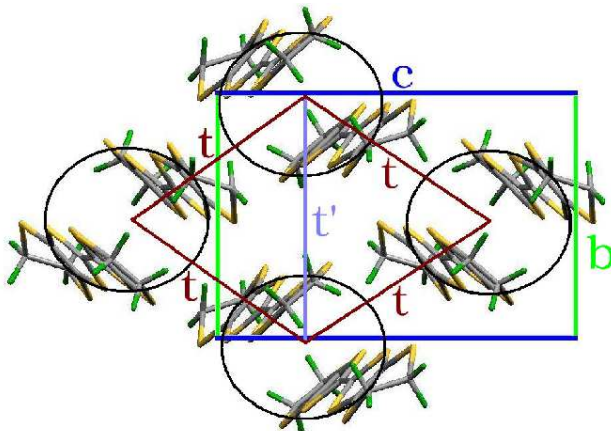


Fig. 1.1. A sketch illustrating why the band structure of the half-filled layered organic charge transfer salts is approximately that of the anisotropic triangular lattice. Black circles indicate the dimers, the hopping integral between the two molecules in a dimer is the largest energy scale in the problem and can be integrated out of the effective low energy Hamiltonian leaving the dimers as effective sites in a Hubbard model description of the electronic degrees of freedom. The largest hopping integrals between the dimers, t and t' , are indicated by the maroon and blue lines. These form an anisotropic triangular lattice. In this review we take the x and y axes of the anisotropic triangular lattice to lie along the directions of the two t hopping integrals as this is conventional in the field. This figure is based on the crystallographic data of Rahal *et al.* for κ -(ET) $_2$ Cu(NCS) $_2$ (a typical half-filled organic charge transfer salt) [26].

S-S or S-C bonds between the two molecules. Rather, the ‘bond’ is between the molecular orbitals themselves, this ‘bond’ results because of the significant overlap between the highest occupied molecular orbitals (HOMOs) on the two molecules, and the fact that the HOMOs are partially occupied. Thus the ‘bond’ between the two molecules forming the dimer is highly analogous to a covalent bond between atoms. The dimer structure is sketched in figure 1.1, also shown are the interdimer hopping integrals. Kino and Fukuyama gave a parameterisation of t and t' , the interdimer hopping integrals, in terms of the intermolecular hopping integrals. It was later realised that this needed to be corrected to allow the strong Coulomb repulsion between two holes on the same molecule [25]. The interdimer hopping integrals form an anisotropic triangular lattice. Thus geometrical frustration may be expected to play a significant role if $t' \sim t$.

The phase diagram of the κ phase materials (the best studied of the half-filled organic charge transfer salts) is sketched in Fig 1.2. It is clear that this phase diagram cannot result from the non-interacting model described above. However, there is a strong Coulombic repulsion between two holes on dimer [27]. Therefore, we believe that the Hubbard model may be the simplest

model which contains the physics required to describe these systems [21, 25]. Kanoda [28] proposed that the role of pressure is to decrease U/W where W is the bandwidth. As different anions lead to different behaviours (and different unit cell volumes) in much the same way as pressure, this can be thought of as an effective ‘chemical pressure’. This idea has proven an extremely powerful framework in which to assimilate the great deal of experimental data now available for these systems.

An often used estimate of U comes from modelling the dimer in a two site Hubbard model with an intermolecular hopping integral, t_m , and a Hubbard repulsion U_m for having two holes on the same *molecule*. In the limit $U_m \gg 4t_m$ this model yields $U \approx 2t_m$ [25]. However, this is rather misleading because quantum chemistry calculations suggest that the Coulomb repulsion between holes on neighbouring molecules in the same dimer V_m is of the order of U_m [27]. Thus this term should be included and therefore the extended (t_m - U_m - V_m) Hubbard model should be used to estimate U [29]. It is straightforward to show [29] that for this model yields

$$U = \frac{1}{2} \left(U_m + V_m - [\{U_m - V_m\}^2 + 16t_m^2]^{1/2} + 4t_m \right) \quad (1.5)$$

and in the appropriate limit, $(U_m + V_m) \gg (U_m - V_m), t_m$, we obtain

$$U \approx \frac{1}{2} (U_m + V_m) \gg 2t_m. \quad (1.6)$$

Taking the values of U_m , V_m and t_m reported by Fortunelli *et al.* [16] we see that equation (1.5) gives $U = 3.7$ eV, this is approximated reasonably well by equation (1.6) which gives $U = 4.8$ eV whereas $2t_m = 0.56$ eV which is the wrong order of magnitude. Thus we see that the plain two site Hubbard (t_m - U_m) model significantly underestimates U . A more detailed discussion of the calculation of the parameters of the Hubbard model will be given in Sect. 1.8.1. In particular that section will discuss the fact that the U *in vacuo* (equation 1.5) is significantly larger than that in the crystal due to the polarisability of the lattice.

The majority of the remainder of this review will be devoted to these half-filled systems. But first we briefly mention three other classes of organic charge transfer salts.

1.2.3 Half-filled charge transfer salts with magnetic anions

An interesting class of organic charge transfer salts have been prepared with magnetic anions. Prominent examples include κ -(BETS)₂FeCl₄ and λ -(BETS)₂FeCl₄. Perhaps the most novel phenomena observed in these salts is field induced superconductivity [31], where superconductivity is not observed at zero field but emerges when a large (> 15 T) field is applied. This occurs due to the Jaccarino-Peter effect [32] which can be described using the

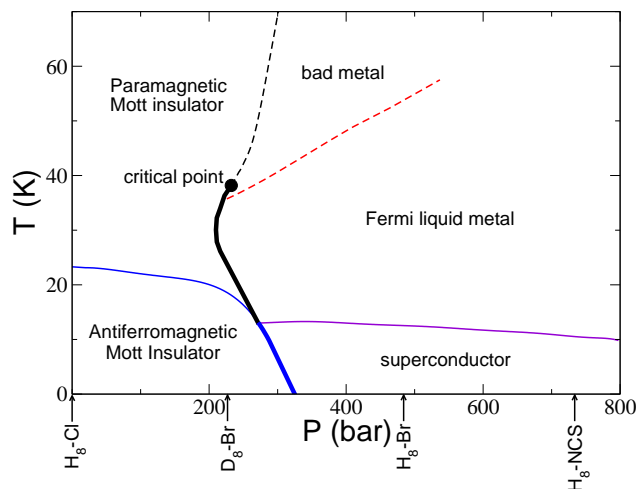


Fig. 1.2. A schematic pressure-temperature phase diagram of κ -(ET) $_2$ X. The first order Mott transition is shown as a thick line, while second order transitions are thin lines and crossovers are dashed lines. The effect ‘chemical’ pressure for different anions, X, is indicated by the arrows on the abscissa. $P = 0$ corresponds to ambient pressure for $X = \text{Cu}[\text{N}(\text{CN})_2]\text{Cl}$ (abbreviated as H₈-Cl in the diagram). H₈-NCS indicates the effective chemical pressure for $X = \text{Cu}(\text{NCS})_2$ (relative to that for $X = \text{Cu}[\text{N}(\text{CN})_2]\text{Cl}$) and H₈-Br indicates the effective chemical pressure for $X = \text{Cu}[\text{N}(\text{CN})_2]\text{Br}$. D₈-Br indicates the effective chemical pressure of $X = \text{Cu}[\text{N}(\text{CN})_2]\text{Br}$ with the ET molecule fully deuterated. (Modified from [30].)

Hubbard-Kondo model [33], in which a Kondo term (to describe the magnetic anions) is added to the Hubbard model described in Sect. 1.2.2. For a recent review of these materials see [34].

1.2.4 Multiband charge transfer salts - the α phase

The α phase salts have a complex band structure in which many bands cross the Fermi level [35]. Thus they cannot be described in the one-band framework which is relevant to the other organic charge transfer salts. These salts have many interesting properties such as charge ordering, an unconventional metallic state and superconductivity [15]. However, space will not permit us to discuss them at length here.

1.2.5 Quasi-one-dimensional charge transfer salts

Finally some organic charge transfer salts, e.g., the Bechgaard and Fabre salt families, are significantly anisotropic in all three directions and are therefore often described as quasi-one-dimensional conductors. Typically the hopping integrals are an order of magnitude larger in intrachain direction than in

the interchain direction, while the interchain hopping integrals are an order of magnitude larger than those interplane [36]. These materials show many interesting behaviours such as spin and charge density waves, superconductivity, possible Luttinger liquid phases, Mott insulating states, spin-Peierls states, antiferromagnetism and Fermi liquid behaviour [37]. A key question is which of the phenomena arise from the quasi-one-dimensionality of the system and for which properties higher dimensional models are required to understand the behaviour.

For the remainder of this review we will discuss the half-filled organic charge transfer salts introduced in section 1.2.2 unless it is explicitly stated otherwise.

1.3 The metallic state

The metallic state is of fundamental importance. Firstly the organic charge transfer salts exhibit an unconventional metallic state which is of great interest in its own right. However, many states of matter occur as instabilities in the metallic state: think, for example, of the Stoner and Cooper instabilities. Thus, for example, the difficulties in understanding the metallic state of the cuprates have greatly compounded the difficulties in explaining the origin of high temperature superconductivity.

Many features of the metallic states of the organic charge transfer salts seem to agree remarkably well with the predictions of dynamical mean field theory (DMFT). In particular, a number of experiments show the features predicted to occur in the crossover from a Fermi liquid to a ‘bad metal’ described by DMFT. However, there remain features of the metallic state that are not well understood. For example, NMR experiments show features consistent with a pseudogap suggesting similarities to the underdoped cuprates (see section 1.8.2). We will only give a very brief discussion of DMFT itself so as to focus on the results and the comparison with experiment. However, both a brief, accessible introduction to DMFT [38] and a more complete technical review [39] are available in the literature.

1.3.1 The bad metal and dynamical mean field theory

The low temperature metallic states of the organic charge transfer salts are exceptionally pure Fermi liquids. This is indicated most clearly by the observation of quantum oscillations and angle-resolved magneto-resistance oscillations (AMRO) [40,41] which demonstrate that the electron transport is coherent (at least within the planes) and that the quasiparticle lifetime is extremely long. At low temperature the resistivity varies like $\rho(T) = \rho_0 + AT^2$ [14, 15, 42, 43], which is the behaviour expected of a Fermi liquid when electron-electron interactions are the dominant scattering mechanism [44, 45].

However, the temperature dependence of the resistivity (shown in figure 1.3) is very different from what is expected for simple metals [where $\rho(T)$ monotonically decreases as T is lowered]. Instead at high temperatures the resistivity *increases* as the temperature is lowered, reaching a broad maximum, and the quadratic temperature dependence is only observed below about 30 K. If the mean free path is less than the lattice spacing it is not meaningful to speak of a coherent wavevector which describes the electronic transport. This condition allows us to define the Mott minimum conductivity [46] (also known as the Mott-Ioffe-Regel limit) which is of order 10^3 S/cm for κ -(ET)₂Cu(NCS)₂. In contrast the conductivity at the peak in the resistivity is ~ 1 S/cm (c.f., Fig 1.3). However, below the peak the resistivity does decrease monotonically, thus this state is described as a ‘bad metal’. Bad metal behaviour is also seen in the alkali doped fullerenes [47], Sr₂RuO₄ [48], SrRuO₃ [49], and VO₂ [50]. All of these systems are strongly correlated materials ‘near to’ a Mott transition. No Drude peak is evident in the optical conductivity of the organic charge transfer salts above about 50 K [51]. Further, even at low temperatures where a ‘Drude-like’ feature does appear, this can only be fit to the Drude form by introducing a frequency dependencies to the scattering rate and the effective mass [51]. On the other hand a broad, high frequency peak is observed at all temperatures. This is suppressed somewhat at low temperatures.

The DMFT of the Hubbard model provides a description of all of this physics [52, 54]. DMFT works by mapping the Hubbard model onto the Anderson model for a single magnetic impurity in a bath of conduction electrons [38, 39]. This procedure is exact in the limits of infinite spatial dimensions or infinite lattice coordination number. For half-filled systems close to a Mott transition DMFT predicts a Fermi liquid at low temperatures, and a crossover to incoherent transport as the temperature is raised. The crossover temperature scale, T_{coh} , is related to the destruction of Kondo screening and Fermi liquid behaviour with increasing temperature (above the Kondo temperature T_K) in the Anderson model. In the Anderson model the conduction electrons are strongly scattered by a (localised) magnetic impurity for $T > T_K$. But for $T < T_K$ a quantum coherent singlet forms between the impurity and the conduction electrons [3]. In the DMFT of the Hubbard model for $T > T_{coh}$ the electrons are quasi-localised and the electrons on the single site treated exactly strongly scatter those in the bath. However, for $T < T_{coh}$ transport is coherent and the electrons only scatter one another weakly, thus Fermi liquid behaviour is regained. This is why, for example, the temperature dependence of the resistivities of the Anderson and Hubbard models are so similar [3, 39]. DMFT predicts that there is no Drude peak in the bad metal phase and that most of the spectral weight is contained in high energy features. This is because much of the spectral weight is transferred to the ‘Hubbard bands’ that will emerge in the Mott insulating state [38, 39]. This prediction is clearly in good agreement with the optical conductivity measurements [51] described above.

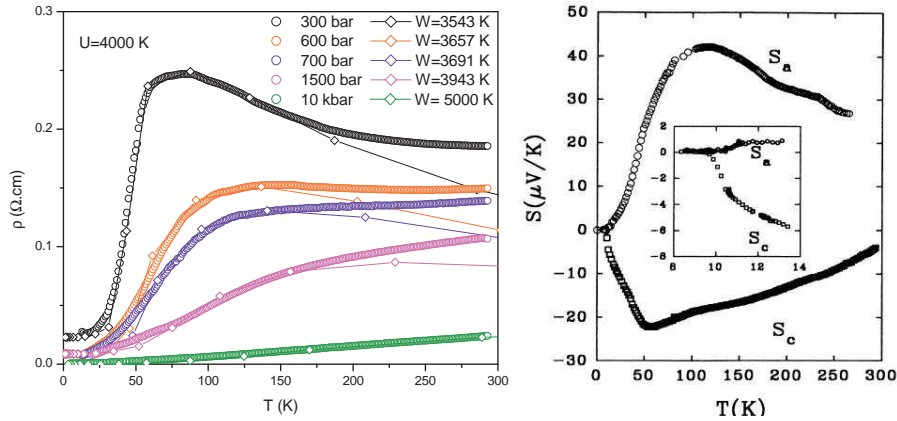


Fig. 1.3. Non-Fermi liquid behaviour in the resistivity and thermopower of half-filled quasi-two-dimensional organic charge transfer salts. The circular data points in the left panel show the non-monotonic temperature dependence of the resistivity, ρ , in κ -(ET) $_2$ Cu[N(CN) $_2$]Cl (to be contrasted with the monotonic behaviour predicted by band theory). At low pressure a broad maximum is observed in the resistivity as is predicted by dynamical mean field theory (DMFT) (shown as rhomboidal data points). As the pressure is increased the broad maximum is suppressed and eventually becomes entirely absent. DMFT reproduces these trends if pressure is taken to control the relative interaction strength ($P \sim W/U$ [28]). This data is taken from [52]. The right panel shows the temperature dependence of the thermopower, S , in the highly conducting plane of κ -(ET) $_2$ Cu[N(CN) $_2$]Br (taken from [53]). The details of the non-interacting band structure dictate that the thermopower is positive when the heat current is parallel to the a -axis and negative when the heat current is parallel to the c -axis. However, along both axes the thermopower has a broad extremum at around the same temperature as the maximum in the resistivity occurs in the left panel. These extrema in the thermopower are predicted by DMFT [54] with $U \sim W$, whereas one expects the thermopower to be monotonic in a system with weakly interacting quasiparticles. Thus these two experiments, which do not have a natural explanation in a Fermi liquid picture are explained by the crossover from a ‘bad metal’ at high temperatures to a Fermi liquid at lower temperatures described by DMFT.

The success of DMFT in describing the transport properties and the phase diagram of many organic charge transfer salts down to temperatures of about 10 K (where, for example, superconductivity becomes important) has been rather puzzling, until recently [11], given that these materials are quasi-two-dimensional and that DMFT is only expected to be a good approximation in the limit of high spatial dimension or high co-ordination number. However, the applicability of DMFT to low-dimensional systems with large frustration is consistent with the fact that for frustrated magnetic models a Curie-Weiss law holds down to a much lower temperature than for unfrustrated models [55,56]. Deviations from Curie-Weiss behaviour result from spatially dependent cor-

relations. Hence, we expect that a DMFT treatment of the Hubbard model on frustrated lattices will be a good approximation down to much lower temperatures than it is for unfrustrated models.

However, DMFT is not simply a theory for describing the conductivity: good agreement with experiment is found for many other properties. For example, measurements of the linear coefficient of the specific heat, γ , of κ -(ET)₂-Cu[N(CN)₂]Br and κ -(ET)₂Cu(NCS)₂ [57] show that the effective mass, m^* , is several (3-5) times that predicted by band theory [58]. Similar effective masses are found in quantum oscillation experiments [40,41]. DMFT predicts this large mass enhancement. This is a result of the strong electronic correlations.

Experimentally, the thermopower, shown in figure 1.3, in the highly conducting (*ac*) plane of κ -(ET)₂Cu[N(CN)₂]Br is positive (negative) in the *a* (*c*) direction.² The thermopower, S , shows a broad maximum (minimum) at around 100 K (60 K) [53], i.e., at about the same temperature the resistivity shows a maximum (figure 1.3). The thermopower predicted for a weakly interacting metallic state with the band structure of κ -(ET)₂Cu[N(CN)₂]Br is ~ 5 times smaller than that observed experimentally [25,53]. DMFT predicts an extremum in the thermopower at $T \sim T_{coh}$ for large U/W [54] and the large effective mass predicted by DMFT gives rise to the large thermopower as $S/T \propto m^*$, in good agreement with experiment.

A strong decrease in the ultrasonic velocity is observed at temperatures ~ 40 K in κ -(ET)₂Cu[N(CN)₂]Br [59], κ -(ET)₂Cu(NCS)₂ [59] and κ -(ET)₂-Cu[N(CN)₂]Cl (under pressure [60]). The pressure (and chemical pressure) dependence of the temperature at which these anomalies are observed show that they occur at the same temperature as the other anomalies that, we have argued above, correspond to T_{coh} . Does this then suggest that phonons play an important role in this physics? DMFT shows that this is not the case. DMFT studies of the Hubbard-Holstein model [61,62] in the limit where the electron-electron interactions are much stronger than the electron-phonon interactions ($U \gg g$) predict phonon anomalies at T_{coh} . However, these anomalies are parasitic: the changes in the behaviour of the electrons cause the change in the behaviour of the lattice vibrations because of the electron-phonon coupling, and the phonons do not play a significant role in driving the crossover from the Fermi liquid to the ‘bad metal’.

The Sommerfeld–Wilson ratio is defined as $R_W = [\chi(T=0)\gamma_0]/(\gamma\chi_0)$, where $\chi(T)$ is the magnetic susceptibility, χ_0 is the zero temperature magnetic susceptibility of the non-interacting electron gas and γ_0 is the linear coefficient of the heat capacity for the non-interacting electron gas. Clearly for the non-interacting system $R_W = 1$, but the Kondo model predicts $R_W = 2$. Therefore, as DMFT exploits the deep connections between Kondo physics and the Mott-

²The sign difference results from the details of the band structure of κ -(ET)₂-Cu[N(CN)₂]Br and corresponds to hole (electron) like conduction along the *a* (*c*) directions [53].

Hubbard transition DMFT predicts $R_W > 1$ in the organics. Experimentally R_W is 1.5 ± 0.2 in both κ -(ET)₂Cu[N(CN)₂]Br and κ -(ET)₂Cu(NCS)₂ [63].

The Kadowaki-Woods ratio is $R_{KW} = A/\gamma^2$, where A is the quadratic coefficient of the resistivity. In many strongly correlated materials $R_{KW} \sim 10.5 \mu\Omega \text{ cm K}^2 \text{ mol}^2 \text{ J}^{-2}$. The Kadowaki-Woods ratio is significantly larger than this in the half-filled layered organic materials, even when differences in the unit cell volume are allowed for [64, 65]. This has led to suggestions that the quadratic temperature dependence of the resistivity may not result from strong electronic correlations, but from phonons [14, 66]. However, one must be careful to allow for the fact that the only reliable resistivity measurements in the organic charge transfer salts are perpendicular to the highly conducting plane. When this is allowed for the observed Kadowaki-Woods ratio is the expected order of magnitude [65].

Collectively the experiments described above (and those studying the Mott transition which we review in section 1.4) show that a weakly interacting, Fermi liquid, description is not sufficient to explain the full temperature dependence of the thermodynamic and transport properties of the half-filled organic charge transfer salts. However, DMFT, which includes the effects of strong electron-electron interactions, and reproduces Fermi liquid theory below T_{coh} , can provide both a quantitative [52] and qualitative [54] description of the full temperature dependence. However, DMFT is a purely local theory. Therefore, any properties with a significant \mathbf{k} -dependence will not be properly described by DMFT. We will discuss some such possible features in section 1.8.2.

1.4 The Mott transition

DMFT also provides a description of the, first order, Mott metal-insulator transition [38, 39]. For $U = 0$ the density of states (DOS) calculated from DMFT is, as one should expect, that of the tight-binding model. For a weakly interacting system the DOS will be only weakly renormalised by the interactions. However, as U is turned on the system becomes strongly interacting and a peak in the DOS will emerge at the Fermi energy. This peak is associated with quasiparticles. The total spectral weight associated with the quasiparticles is $Z = m_b/m^* < 1$, where m_b is the band mass of the electron, hence Z is called the quasiparticle weight. The remainder of the spectral weight is transferred to two broad bands centred on $\pm U/2$ of width $\sim W$, known as the Hubbard bands. The Hubbard bands correspond to quasi-localised states with the lower Hubbard band (centred at $-U/2$) corresponding to singly occupied sites and the upper Hubbard band (centred at $+U/2$) corresponding to doubly occupied sites. As U is further increased the quasiparticle peak narrows (Z decreases) and more spectral weight is transferred to Hubbard bands. When U is increased above the critical $U \sim W$ for the Mott transition the quasiparticle peak vanishes and all of the spectral weight resides in the Hubbard

bands. There is now no density of states at the Fermi energy and so we have an insulator. A number of studies have found that this transition is first order within the DMFT framework [39, 67].

It is conceptually useful to compare the Mott transition in the organic charge transfer salts (figure 1.2) and that predicted for the Hubbard model on the anisotropic triangular lattice by DMFT with the liquid-gas transition. The difference between the liquid and the gas is their densities. One may move from the gas to the liquid in either of two ways: either directly, by increasing the pressure through a first order phase transition where the density changes discontinuously; or by first increasing the temperature above the critical temperature and then passing around the critical point. If one passes around the critical point no phase transition is observed and the density varies continuously through the fluid phase. The Mott transition behaves in much the same way. In the Mott insulator the electrons are localised and hence the conductivity is poor whereas the metal has a large conductivity. We may either drive the Mott transition by increasing the pressure and passing directly through the first order transition where the degree of localisation changes discontinuously, or else we may first increase the temperature above the critical temperature where the line of first order transitions ends (see figure 1.2) and thus pass continuously from the insulating phase to the metallic phase. In this picture the ‘bad-metal’ is somewhat analogous to the fluid. As we move through the ‘bad-metal’ the conductivity changes continuously as we pass from the localised behaviour of the insulator to the coherent excitations characteristic of the Fermi liquid. Although one should note that the analogy is not exact as the ‘bad metal’ regime extends slightly below the critical point (c.f. figure 1.2).

1.4.1 The critical point

We now turn our discussion to the critical point itself. Unsurprisingly, DMFT predicts mean-field critical exponents (see table 1.1). Limelette *et al.* [68] measured the critical exponents of the Mott transition in V_2O_3 [68].³ They

³These exponents can be measured by studying the conductivity near the Mott transition. The conductivity gives access to the critical behaviour as it is related to the thermodynamic ground state via linear response theory. The critical exponents can be determined from the conductivity, σ , as: $(\sigma - \sigma_c) \sim (T_c - T)^\beta$, $(d\sigma/dP)_T \sim |T - T_c|^{-\gamma}$ and $(\sigma - \sigma_c) \sim (P - P_c)^{1/\delta}$, where σ_c is the conductivity at the critical point, T is the temperature, T_c is the critical temperature, P is the pressure and P_c is the critical pressure. To interpret the order parameter exponent on the critical isotherm, δ , one should recall that the order parameter of the Mott transition is the half-width of the coexistence curve, which vanishes at the critical point. This is entirely analogous to the liquid-gas transition [69]. It is often stated that the order parameter of the liquid-gas transition is the difference in the densities of the liquid and the gas. This statement needs to be interpreted carefully. Strictly the density difference between the liquid and the gas phase *when they are in coexistence*

	Example system	β	γ	δ
mean field [69]	DMFT	1/2	1	3
3D Ising [69]	Liquid-gas	0.33	1.24	4.8
3D XY	Superconductor	0.35	1.3	4.8
3D Heisenberg	Ferromagnet	0.36	1.4	4.8
2D Ising [69]	Physisorption	1/8	7/4	15
mean field at MQCP	MQCP [71, 72]	1	1	2
mean field near MQCP	MQCP [72]	1 \rightarrow 0.33	1 \rightarrow 1.24	2 \rightarrow 4.8
3D metal-insulator	V ₂ O ₃ [68]	0.34 \rightarrow 0.5	1	5 \rightarrow 3
2D metal-insulator?	κ -(ET) ₂ Cu[N(CN) ₂]Cl [70]	0.9-1	0.9-1	1.9-2

Table 1.1. Comparison of the critical exponents observed for some common universality classes with those seen at the critical point of the Mott transition in κ -(ET)₂-Cu[N(CN)₂]Cl. The symbol $X \rightarrow Y$ indicates that the measured exponent crosses over from X in a small critical region near the critical point, to Y in a larger region further from the critical point.

observed three dimensional (3D) Ising exponents (the same as are seen in the liquid-gas transition), but only in an extremely narrow critical region around the critical point ($P/P_c, T/T_c \lesssim 10^{-2}$). Limelette *et al.* observed mean-field critical exponents except in this extremely small critical region near the critical point which, they argued, implies that there are bound pairs of doubly occupied and vacant sites near the Mott transition. These bound states can exist over large length scales (of order nm) and are argued to be the root cause of the success of DMFT. This is analogous to the success of the (mean field) BCS theory of superconductors which results from the large coherence length (and hence small critical region) in conventional superconductors.

However, recently Kagawa *et al.* [70] have found that the critical exponents for the critical end point of the Mott transition in κ -(ET)₂Cu[N(CN)₂]Cl do not correspond to either the Ising or mean field universality classes. Indeed the critical exponents do not belong to any universality class that had previously been observed (see table 1.1). Crucially, in spite of being very different from those for the Ising, XY or Heisenberg universality classes, the observed exponents obey the standard scaling relation $(\delta - 1)\beta = \gamma$, within experimental error.

Remarkably, Imada [71] had predicted these exponents from phenomenological theories of the Mott transition. Misawa *et al.* [72] have now shown that these critical exponents may be derived within the Hartree-Fock approximation from the Hubbard model on the anisotropic triangular lattice. Within the Hartree-Fock approximation the metal becomes magnetically ordered at

is a good order parameter. This is, of course, proportional to the half-width of the coexistence curve because of the Maxwell equal area construction. However, the density difference when the liquid and gas when they are not in coexistence is *not* a good order parameter. These comments are equally valid for the difference in conductivities between the metal and insulator in the Mott transition.

relatively small U/W . But the metal insulator transition does not occur until $U \sim W$. Thus there is no symmetry breaking at the metal-insulator transition within the Hartree-Fock approximation. Misawa *et al.* find that for $0.056 \approx t'_{c1}/t < t'/t < t'_{c2}/t \approx 0.365$ a line of first order phase transitions ends at a finite temperature critical point. At t'_{c1} and t'_{c2} this critical point is driven to $T = 0$ and for $t'/t < t'_{c1}/t$ or $t'/t > t'_{c2}/t$ a quantum critical point is observed. $t' = t'_{c1}$ and $t' = t'_{c2}$ are therefore termed marginal quantum critical points (MQCPs). At the MQCPs Misawa *et al.* find that the critical exponents are $\beta = 1$, $\gamma = 1$ and $\delta = 2$, which satisfy the scaling relation $(\delta - 1)\beta = \gamma$, and agree with those measured by Kagawa *et al.* [70] in κ -(ET)₂Cu[N(CN)₂]Cl within experimental error. However, one should recall that these exponents are only strictly valid at $T = 0$ and the critical point in κ -(ET)₂Cu[N(CN)₂]Cl occurs at 39.7 K - where we might expect to regain the standard Ising critical exponents. However, Misawa *et al.* stress that the true critical exponents will only apply within a small critical region very close to the phase transition and that beyond that region the observed exponents will crossover to those characteristic of the MQCP. Misawa *et al.* estimate that experimental resolution of Kagawa *et al.* is two orders of magnitude worse than that required to see the Ising critical behaviour. Misawa *et al.* stress that the fact that magnetic order exists on both the insulating and metallic sides of the phase transition is vital for their theory.⁴ We should note that that in κ -(ET)₂Cu[N(CN)₂]Cl antiferromagnetic ordering does not occur over the entirety of the Mott insulating phase, but only at low temperatures (see figure 1.2). Therefore, the Mott transition in κ -(ET)₂Cu[N(CN)₂]Cl is not accompanied by any symmetry breaking in the vicinity of the critical point. Importantly, the Ginzburg criterion shows that the upper critical dimension is two and so the mean field Hartree-Fock treatment, which neglects all fluctuations, appears likely to be correct in cases where no symmetry is broken at the critical point. It is important to note the role that frustration plays in this scenario as for weakly frustrated lattices ($t'/t < t'_{c1}/t$ or $t'/t > t'_{c2}/t$) these unconventional critical exponents are not predicted.

1.5 The superconducting state

The organic charge transfer salts are often referred to as the organic superconductors. However, this is somewhat misleading both because of the range of other phenomena observed in the organic charge transfer salts and because of the range of other materials which fit the description ‘organic superconductors’. Other organic superconductors include the alkali doped fullerenes [47], intercalated graphite [73] and ion implanted polymers [74]. However, below we

⁴Note that Imada’s [71] phenomenological theories which predict the same exponents do so in the case of the non-magnetic-insulator to non-magnetic-metal transition.

discuss only superconductivity in the quasi-two-dimensional half-filled organic charge transfer salts.

The phrase ‘unconventional superconductivity’ has several meanings. These meanings are best illustrated by comparison to elemental superconductors, which are described by BCS theory [4] (or more accurately by Eliashberg theory [75] or the density functional theory of superconductivity [76]). In these theories the electrons form Cooper pairs due to an effective attractive interaction between electrons mediated by the exchange of phonons. The BCS state breaks gauge symmetry but no other symmetry of the crystal. Thus the phrase ‘unconventional superconductivity’ can be applied to any superconductor that does not satisfy any one of these three requirements (BCS, phononic pairing mechanism and no additional symmetry breaking) for conventional superconductivity. In this section we review the experimental evidence which shows that the superconductivity in the half-filled organic charge transfer salts is unconventional in all three of the senses described above. We delay a detailed discussion of the theory until section 1.6.

1.5.1 Pairing symmetry (evidence for additional symmetry breaking)

In the original formulation of BCS theory [4] one assumes that the effective attractive pairwise interaction responsible for superconductivity, V , is spatially uniform. This means that the superconducting order parameter Δ is also isotropic as $\Delta = \sum_{\mathbf{k}} V \langle c_{\mathbf{k}\uparrow} c_{-\mathbf{k}\downarrow} \rangle$. This assumption is somewhat unphysical, but it is straightforward to generalise BCS theory to allow for momentum dependent effective interactions, $V_{\mathbf{k}}$ [77]. In this case we should also allow the order parameter to develop a \mathbf{k} -dependence by defining $\Delta_{\mathbf{k}} = \sum_{\mathbf{k}'} V_{\mathbf{k}-\mathbf{k}'} \langle c_{\mathbf{k}'\uparrow} c_{-\mathbf{k}'\downarrow} \rangle$. It is now natural to ask what symmetry $\Delta_{\mathbf{k}}$ has. Note that although we have introduced these ideas in the context of BCS theory the symmetry arguments that follow are based basic truths about quantum mechanics and do not depend on the details of the microscopic theory of superconductivity. Thus symmetry analyses are a powerful framework in which to understand the phenomenology of unconventional superconductors [7, 24, 78].

A brief introduction to the symmetry of pairing states

A fundamental theorem of quantum mechanics is that the eigenstates must transform according to an irreducible representation of the symmetry group of the Hamiltonian [79].⁵ This is true regardless of the complexity of the quantum

⁵Here we neglect the possibility of accidental degeneracies as they complicate the discussion considerably, but do not really change the physics as the accidentally degenerate states can always be decomposed into a set of eigenstates that transform under the operations of the group in the same way as a set of the irreducible representations of the symmetry group of the Hamiltonian.

many-body Hamiltonian. Therefore, one expects on very general grounds that the superconducting order parameter (which has the same symmetry as the wavefunction describing the superconducting state⁶) will have the symmetry of a particular irreducible representation of the group describing the symmetry of the normal state (and hence the Hamiltonian at T_c). This argument can be made rigorous exactly at the critical temperature, and may be expected to hold below T_c provided there are no further phase transitions.

In elemental superconductors it is found that, although $\Delta_{\mathbf{k}}$ is not completely isotropic [80] the order parameter does have the same symmetry as the crystal. The first material found where this did not appear to be the case was in superfluid ^3He . Clearly there is no crystal in liquid ^3He and so the normal state has the full symmetry of free space. Therefore, the expectation that the order parameter will transform like a particular representation of the group describing the symmetry of the normal state can be recast as the claim that if we expand the order parameter in terms of the spherical harmonics, $Y_{lm}(\hat{\mathbf{k}})$,

$$\Delta_{\mathbf{k}} = \sum_{l=0}^{\infty} \sum_{m=-l}^l \eta_{lm} Y_{lm}(\hat{\mathbf{k}}), \quad (1.7)$$

then we will find that we only require η_{lm} to be finite for one particular value of l . Thus we find that

$$\Delta_{\mathbf{k}} = \sum_{m=-l}^l \eta_{lm} Y_{lm}(\hat{\mathbf{k}}). \quad (1.8)$$

It is natural to refer to superconductors in which the non-zero η_{lm} are $l = 0$ as *s*-wave, superconductors in which the finite η_{lm} are $l = 1$ as *p*-wave, superconductors in which the finite η_{lm} are $l = 2$ as *d*-wave, and so on, by analogy with atomic physics. It has been established that ^3He is a *p*-wave superconductor [81].

Historically, the discovery that superfluid ^3He has a lower symmetry than normal ^3He preceded any analogous discoveries in superconductors by some time. However, there are now several materials in which the superconducting state is believed to have a lower symmetry than the normal state. These include, Sr_2RuO_4 , the cuprates, several heavy fermion materials and, we will argue below the layered organic charge transfer salts. One often hears statements such as “the cuprates are *d*-wave superconductors”. It is not immediately clear what this means as the normal state of the cuprates does not have the full symmetry of free space (due to the crystal lattice) and so the spherical harmonics are not an appropriate basis in which to expand the order parameter.

⁶Assuming no other phase transition accompanies the superconducting transition.

In a crystal the natural basis is that of the irreducible representations of the point group of the crystal.⁷ (Table 1.2 describes the point group D_{4h} which is that of most cuprates and a number of other unconventional superconductors and tables 1.3-1.5 give three examples of point groups relevant to the organic charge transfer salts.) In this case the order parameter may be written as

$$\Delta_{\mathbf{k}} = \sum_{i=0}^{d^F} \eta_i \psi_i^F(\mathbf{k}), \quad (1.9)$$

where $\psi_i^F(\mathbf{k})$ are the basis functions of the F^{th} irreducible representation and d^F is the dimension of F .

The above discussion is only valid for singlet superconductors. Triplet superconductivity does not greatly complicate this analysis, but one does have to include a sum over the three spin projections of the $S = 1$ Cooper pairs and generalise the order parameter slightly (see [7], [78] or [82] for a careful discussion of the group theoretic classification of triplet states).

Thus when the statement is made that “the cuprates are $d_{x^2-y^2}$ superconductors”, what is meant is that the superconducting state transforms like the B_{1g} representation of the group D_{4h} (c.f. table 1.2). However, all possible basis functions of the B_{1g} representation of D_{4h} vanish along the lines $k_x = \pm k_y$. Thus the nodes of the order parameter (which are often all one is concerned with, see below and section 1.5.2) are the same as for the $d_{x^2-y^2}$ spherical harmonic. Thus in analogy with the case of ^3He , people often refer to ‘s-wave’, ‘p-wave’ or ‘d-wave’ superconductors. One should always bare in mind what this naming conventional really means, as confusion can arise (and repeatedly has arisen) when the terms are used carelessly. However, this terminology is all but universal and therefore we will make use of it, but we will use inverted commas to remind the reader that an analogy is being drawn and that we really mean a particular irreducible representation of the point group of the crystal in question.

Singlet or triplet?

As all of the half-filled organic charge transfer salts have inversion symmetry singlet and triplet states are distinct [78]. Thus the first question we should ask is whether the superconducting states of these materials are singlet or triplet. Measurements of the ^{13}C NMR Knight shift [83–85] in $\kappa\text{-(ET)}_2\text{Cu-[N(CN)}_2\text{]Br}$, with the magnetic field, \mathbf{H} , parallel to the conducting planes, show that as $T \rightarrow 0$ so does the Knight shift. This single experiment does not actually rule out triplet pairing, although it does make triplet pairing extremely unlikely. This experiment is compatible with a triplet state in which $\mathbf{d}(\mathbf{k}) \times \mathbf{H} = 0$ where $\mathbf{d}(\mathbf{k})$ is the usual Balian–Werthamer order parameter

⁷We assume throughout that the superconducting state does not break translational symmetry.

Irrep	E	C_4^c	$C_2^{a/b}$	C_2^d	C_2^c	i	S_4^c	σ_{bc}^{ac}	σ^{dc}	σ^{ab}	Required nodes	Example basis functions	Colloquial names
A_{1g}	1	1	1	1	1	1	1	1	1	1	none	$1_{\mathbf{k}}, X_{\mathbf{k}}^2 + Y_{\mathbf{k}}^2, Z_{\mathbf{k}}^2$	s
A_{2g}	1	1	-1	-1	1	1	1	1	-1	-1	line	$X_{\mathbf{k}}Y_{\mathbf{k}}(X_{\mathbf{k}}^2 - Y_{\mathbf{k}}^2)$	g
B_{1g}	1	-1	-1	1	1	1	1	-1	1	-1	line	$X_{\mathbf{k}}^2 - Y_{\mathbf{k}}^2$	$d_{x^2-y^2}$
B_{2g}	1	-1	1	-1	1	1	1	-1	-1	1	line	$X_{\mathbf{k}}Y_{\mathbf{k}}$	d_{xy}
E_g	2	-2	0	0	0	2	-2	0	0	0	none	$(X_{\mathbf{k}}Z_{\mathbf{k}}, Y_{\mathbf{k}}Z_{\mathbf{k}})$	(d_{xz}, d_{yz})
A_{1u}	1	1	1	1	1	-1	-1	-1	-1	-1	none	$X_{\mathbf{k}}^2Y_{\mathbf{k}}^2Z_{\mathbf{k}}$	h
A_{2u}	1	1	-1	-1	1	-1	-1	-1	1	1	line	$Z_{\mathbf{k}}$	p_z
B_{1u}	1	-1	-1	1	1	-1	-1	1	-1	1	line	$X_{\mathbf{k}}Y_{\mathbf{k}}Z_{\mathbf{k}}$	f_{xyz}
B_{2u}	1	-1	1	-1	1	-1	-1	1	1	-1	line	$(X_{\mathbf{k}}^2 - Y_{\mathbf{k}}^2)Z_{\mathbf{k}}$	$f_{(x^2-y^2)z}$
E_u	2	-2	0	0	0	-2	2	0	0	0	none	$(X_{\mathbf{k}}, Y_{\mathbf{k}})$	(p_x, p_y)

Table 1.2. The character table, symmetry required nodes in the superconducting energy gap and some basis functions of the irreducible representations of the point group D_{4h} . This is the point group of many unconventional superconductors with tetragonal crystals, including many of the cuprates and Sr_2RuO_4 . We assume that the x , y and z axes are, respectively, parallel to the a , b and c axes. The functions $1_{\mathbf{k}}$, $X_{\mathbf{k}}$, $Y_{\mathbf{k}}$ and $Z_{\mathbf{k}}$ may be any functions which transform, respectively, as 1, k_x , k_y and k_z under the operations of the group and satisfy translational symmetry. The operations of the group are the identity (E), rotation by π and $\pi/2$ about the c axis (respectively C_2^c and C_4^c), rotation by π about the a and b axes (which have the same characters, which we therefore label $C_2^{a/b}$), rotation by π about the either of the diagonal of the a - b plane (which have the same characters and are labelled C_2^d), inversion (i : inversion symmetry takes \mathbf{k} to $-\mathbf{k}$), an improper by $\pi/4$ about the c axis (S_4^c : an improper is a rotation followed by a reflection through the plane perpendicular to the axis of rotation), reflection through the ab plane (σ^{ab}) reflection through the ac and bc planes (which have the same characters, which we therefore label σ_{bc}^{ac}) and reflection through the planes specified by $(x+y)z=0$ and $(x-y)z=0$ (which have the same characters and are labelled σ^{dc}). A brief explanation of characters is given in the caption to table 1.3.

for triplet superconductivity [82, 86]. However, Zuo *et al.* [87] measured the critical field as a function of temperature with \mathbf{H} parallel to the conducting planes. In this configuration no orbital currents flow so the critical field is due to Clogston–Chandrasekhar (or Pauli) limit [88–90]. There is no Clogston–Chandrasekhar limit for $\mathbf{H} \perp c$ for triplet states compatible with measured Knight shift. Thus, for such states there would be no critical field with $\mathbf{H} \parallel b$ (in fact for such states one would increase T_c by applying a field parallel to the b -axis [90]). Experimentally [91] it is found that superconductivity is destroyed by a magnetic field parallel to the b -axis. Therefore, only when considered together do the three experiments discussed above [83, 87, 91] strictly rule out triplet pairing. Further evidence for Clogston–Chandrasekhar limiting, and hence singlet pairing, comes from the observation that the in plane upper critical field is independent of the field direction [92]. Given the anisotropic nature of the Fermi surface of κ -(ET) $_2$ Cu[N(CN) $_2$]Br it is extremely unlikely

Irrep	E	C_2^a	C_2^b	C_2^c	i	σ^{bc}	σ^{ac}	σ^{ab}	Required nodes	Example basis functions	Colloquial names
A_{1g}	1	1	1	1	1	1	1	1	none	$1_{\mathbf{k}}, A_{\mathbf{k}}^2, B_{\mathbf{k}}^2, C_{\mathbf{k}}^2, X_{\mathbf{k}}Y_{\mathbf{k}}$	s (d_{xy})
B_{1g}	1	-1	-1	1	1	-1	-1	1	line	$A_{\mathbf{k}}B_{\mathbf{k}}, (X_{\mathbf{k}} + Y_{\mathbf{k}})Z_{\mathbf{k}}$	$d_{(x+y)z}$
B_{2g}	1	-1	1	-1	1	-1	1	-1	line	$A_{\mathbf{k}}C_{\mathbf{k}}, X_{\mathbf{k}}^2 - Y_{\mathbf{k}}^2$	$d_{x^2-y^2}$
B_{3g}	1	1	-1	-1	1	1	-1	-1	line	$B_{\mathbf{k}}C_{\mathbf{k}}, (X_{\mathbf{k}} - Y_{\mathbf{k}})Z_{\mathbf{k}}$	$d_{(x-y)z}$
A_{1u}	1	1	1	1	-1	-1	-1	-1	none	$A_{\mathbf{k}}B_{\mathbf{k}}C_{\mathbf{k}}, (X_{\mathbf{k}}^2 - Y_{\mathbf{k}}^2)Z_{\mathbf{k}}$	f
B_{1u}	1	-1	-1	1	-1	1	1	-1	line	$C_{\mathbf{k}}, X_{\mathbf{k}} + Y_{\mathbf{k}}$	$p_{(x-y)}$
B_{2u}	1	-1	1	-1	-1	1	-1	1	line	$B_{\mathbf{k}}, Z_{\mathbf{k}}$	p_z
B_{3u}	1	1	-1	-1	-1	-1	1	1	line	$A_{\mathbf{k}}, X_{\mathbf{k}} - Y_{\mathbf{k}}$	$p_{(x+y)}$

Table 1.3. The character table, symmetry required nodes in the superconducting energy gap and some basis functions of the irreducible representations of the point group D_{2h} . This is the symmetry of the orthorhombic organic superconductors such as κ -(ET) $_2$ Cu[N(CN) $_2$]Br. We argue in section 1.5 that the experimental evidence (see Figs. 1.4 and 1.5) shows that the superconducting order parameters of κ -(ET) $_2$ -Cu[N(CN) $_2$]Br and other orthorhombic organic charge transfer salts transform like the B_{2g} representation of D_{2h} . Thus the superconducting state may be said to be ‘ $d_{x^2-y^2}$ ’. In the colloquial names column we include d_{xy} , parenthetically, as a name for the A_{1g} representation. This is not intended to encourage the use of this name but merely to stress that order parameters transforming like the B_{2g} representation of D_{4h} (which have been invoked to explain some experimental data; see, e.g. [93]) transform according to the A_{1g} representation of D_{2h} and are therefore are not symmetry distinct from ‘ s -wave’ order parameters. Note that in κ -(ET) $_2$ Cu[N(CN) $_2$]Br the highly conducting plane is the a - c plane, and that the x and y axes are taken to lie along the same directions as the t hopping integrals (c.f., figure 1.1) therefore $k_a = k_x + k_y$ and $k_c = k_x - k_y$. The functions $1_{\mathbf{k}}, X_{\mathbf{k}}, Y_{\mathbf{k}}, Z_{\mathbf{k}}, A_{\mathbf{k}}, B_{\mathbf{k}}$ and $C_{\mathbf{k}}$ may be any functions which transform, respectively, as $1, k_x, k_y, k_z, k_a, k_b$ and k_c under the operations of the group and satisfy translational symmetry. The operations of the group are the identity (E), rotation by π about the a, b and c axes (respectively C_2^a, C_2^b and C_2^c), inversion (i) and reflection through the ab, ac and bc planes (respectively σ^{ab}, σ^{ac} and σ^{bc}). The character is the trace of any matrix that can represent the operation in that irreducible representation (see [79] for a detailed discussion). However, for the one-dimensional representations relevant here the character has more physical interpretation: the character is the sign introduced in the order parameter (and wavefunction) by that operation. For example, any order parameter transforming according to the A_{1g} representation will be unchanged by any of the operations of the group. On the other hand if the order parameter transforms according to the B_{2g} representation (as does, for example, $\Delta_k \sim \cos k_x - \cos k_y$) then the order parameter changes sign under rotation by π about the a ($x+y$) or c ($x-y$) axes and reflection through the bc ($x=y$) and ab ($x=-y$) planes.

that orbital mechanisms for the destruction of superconductivity would be so isotropic.

Spatial symmetry ('s-wave' versus 'd-wave')

The organic charge transfer salts form orthorhombic, monoclinic and triclinic crystals. This can lead to important differences between their superconducting states [24, 94]. Orthorhombic crystals such as κ -(ET)₂Cu[N(CN)₂]Br (in which the highly conducting plane is the *a-c* plane) are described by the D_{2h} point group. There are four irreducible representations of D_{2h} which correspond to singlet superconductivity (see table 1.3). Given the layered structure of the crystals superconductivity transforming as either the B_{1g} or B_{3g} irreducible representations is unlikely [24, 78]. Therefore, our task is to differentiate between superconducting order parameters transforming like the A_{1g} representation (which is often referred to as 's-wave' superconductivity) and superconducting states that transform according to the B_{2g} representation (or ' $d_{x^2-y^2}$ ' superconductivity).

There are even less symmetry distinct superconducting states in monoclinic crystals such as κ -(ET)₂Cu(NCS)₂ (for which the highly conducting plane is the *b-c* plane) which are described by the C_{2h} point group. There are two irreducible representations of C_{2h} which correspond to singlet superconductivity (see table 1.4). Therefore, the singlet order parameter must transform like either the A_g representation (which we may refer to as 's-wave' superconductivity) or the B_g representation (which we may refer to as 'd-wave' superconductivity⁸).

One way to differentiate between 's-wave' and 'd-wave' states⁹ is to measure the *low temperature* behaviour of thermodynamic variables. For an 's-wave' state the superconducting gap is finite at every point on the Fermi surface. As excitations may only take place at energies within about $k_B T$ of the Fermi energy thermodynamic properties are exponentially activated at low temperatures. For example, the heat capacity $C_v \propto \exp(-\Delta_0/k_B T)$ for $T \ll T_c$, where Δ_0 is the minimum value of the magnitude of the superconducting gap at the Fermi surface at $T = 0$. In contrast for a ' $d_{x^2-y^2}$ ' state symmetry requires that the superconducting order parameter vanishes along (at) four lines (points) on a three (two) dimensional Fermi surface. These lines (points) are known as nodes. At the nodes there are excitations with arbitrarily low energies. Thus although density of states, $D(\epsilon)$, does vanish at the Fermi energy, ϵ_F , in a 'd-wave' superconductor, the DOS grows linearly as we move away from the Fermi energy, $D(\epsilon) \propto |\epsilon - \epsilon_F|$ for $|\epsilon - \epsilon_F| \ll |\Delta|$. As, for example, $C_v/T \sim D(\epsilon)$ it follows that at *low temperatures* $C_v \propto T^2$ in a 'd-wave' superconductor.

Measurements of the temperature dependence of the heat capacity [13], penetration depth [95] and nuclear spin lattice relaxation rate [83–85] have

⁸Although the only symmetry required node for states transforming according to the B_g representation lies along the *c*-axis [24] and so such states will not, in general, be the same as the ' $d_{x^2-y^2}$ ' state described above

⁹From hereon we use the phrase 'd-wave' to refer to both the B_g representation of C_{2h} and the B_{2g} representation of D_{2h} unless we explicitly state otherwise.

Irrrep	E	C_2^c	i	σ^{ab}	Required nodes	Example basis functions	Colloquial names
A_g	1	1	1	1	none	$1_{\mathbf{k}}, A_{\mathbf{k}}^2, B_{\mathbf{k}}^2, C_{\mathbf{k}}^2, X_{\mathbf{k}}Y_{\mathbf{k}}$	s (d_{xy})
B_g	1	-1	1	-1	line	$A_{\mathbf{k}}C_{\mathbf{k}}, (X_{\mathbf{k}} - Y_{\mathbf{k}})Z_{\mathbf{k}}, B_{\mathbf{k}}C_{\mathbf{k}}, X_{\mathbf{k}}^2 - Y_{\mathbf{k}}^2$	d
A_u	1	1	-1	-1	none	$A_{\mathbf{k}}, B_{\mathbf{k}}, X_{\mathbf{k}} + Y_{\mathbf{k}}$	p_{x+y}
B_u	1	-1	-1	1	line	$C_{\mathbf{k}}, X_{\mathbf{k}} - Y_{\mathbf{k}}$	p_{x-y}

Table 1.4. The character table, symmetry required nodes and some basis functions of the even parity irreducible representations of the point group C_{2h} . This represents the symmetry of the monoclinic organic superconductors such as κ -(ET) $_2$ Cu(NCS) $_2$. We argue in section 1.5 that the experimental evidence (see Figs. 1.4 and 1.5) shows that the superconducting order parameters of κ -(ET) $_2$ Cu(NCS) $_2$ and other monoclinic organic charge transfer salts transform like the B_g representation of C_{2h} . Thus the superconducting state may be said to be ‘ d -wave’. In the colloquial names column we include d_{xy} , parenthetically, as a name for the A_{1g} representation. This is not intended to encourage the use of this name but merely to stress that order parameters transforming like the B_{2g} representation of D_{4h} (which have been invoked to explain some experimental data; see, e.g. [93]) transform according to the A_{1g} representation of C_{2h} are therefore are not symmetry distinct from ‘ s -wave’ order parameters. Note that in κ -(ET) $_2$ Cu(NCS) $_2$ the highly conducting plane is the b - c plane, and that the x and y axes are taken to lie along the same directions as the t hopping integrals (c.f., figure 1.1) therefore $k_b = k_x + k_y$ and $k_c = k_x - k_y$. The functions $1_{\mathbf{k}}, X_{\mathbf{k}}, Y_{\mathbf{k}}, Z_{\mathbf{k}}, A_{\mathbf{k}}, B_{\mathbf{k}}$ and $C_{\mathbf{k}}$ may be any functions which transform, respectively, as 1, k_x, k_y, k_z, k_a, k_b and k_c under the operations of the group and satisfy translational symmetry. A brief explanation of characters is given in the caption to table 1.3.

produced apparently rather contradictory results; with some groups arguing that their results provide evidence for fully gapped ‘ s -wave’ pairing and other groups arguing that their data favours states with nodes such as ‘ d -wave’ superconductivity. (We recently reviewed this data in rather more detail in [96].) However, it is important to note that many of these experiments were not performed in the $T \ll T_c$ limit and therefore do not strongly differentiate between exponentially activated and power law behaviours. The only experiment, which we are aware of, reporting data below about 20% of T_c is the penetration depth, λ , study of Carrington *et al.* [95] which reports data down to about 1% of T_c . They found a power law behaviour, but with a peculiar $\lambda(T) - \lambda(0) \propto T^{3/2}$ behaviour¹⁰ (see figure 1.5). The correct interpretation of this temperature dependence is not clear at the current time, except to note that their data is quite inconsistent with an ‘ s -wave’ order parameter.

In the cuprates phase sensitive probes, especially tunnelling [98] and scanning tunnelling microscopy (STM) [99] experiments have been particularly important for determining the pairing symmetry. However, such experiments

¹⁰One expects $\lambda(T) - \lambda(0) \propto T$ for line (point) nodes and a three- (two-) dimensional Fermi surface and $\lambda(T) - \lambda(0) \propto T^2$ for point nodes on a three-dimensional Fermi surface [7].

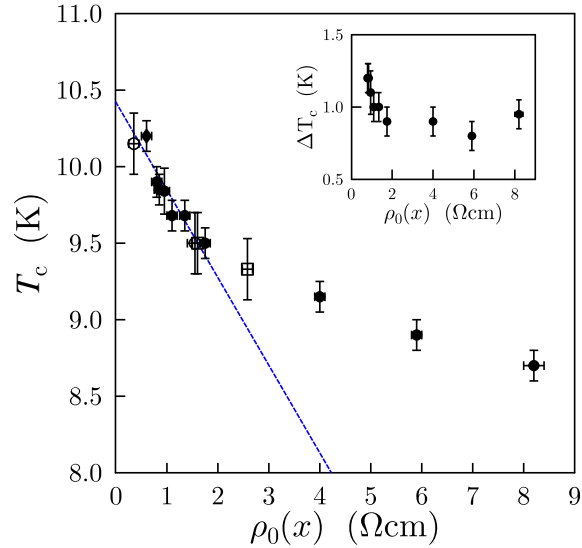


Fig. 1.4. Experimental evidence for unconventional superconductivity in half-filled quasi-two-dimensional organic charge transfer salts from measurements of suppression of T_c by disorder (taken from [43]). It shows the variation of the critical temperature, T_c , and residual resistivity, ρ_0 , of κ -(ET) $_2$ Cu(NCS) $_2$ as disorder is introduced by irradiating the sample. The line shows the prediction of the Abrikosov-Gorkov theory (1.10) for a ‘non- s -wave’ superconducting order parameter (that transforms as a non-trivial representation). In contrast for an ‘ s -wave’ order parameter Anderson’s theorem [97] predicts that the critical temperature is not suppressed by low levels of disorder. Thus, the strong initial suppression of T_c as ρ_0 (which is inversely proportional to the electron-impurity scattering rate) increases is strongly suggestive of a ‘non- s -wave’ order parameter. However, it is not currently understood why T_c is greater than is predicted by the Abrikosov-Gorkov theory for $\rho_0 \gtrsim 2 \Omega\text{cm}$.

have not been reliably performed in the organic charge transfer salts (see [96] for a critical review of the experiments that have been performed to date.)

An important distinction between ‘ s -wave’ superconductors and ‘non- s -wave’ superconductors is the effect of non-magnetic disorder. When a quasiparticle is scattered by a non-magnetic impurity its momentum is changed by a random amount. However, Fermi statistics dictate that quasiparticles may only scatter from and to states near the Fermi surface. Therefore, in a superconductor impurity scattering has the effect of averaging the order parameter over the Fermi surface [96, 100]. For states transforming as the trivial representation (e.g., the A_{1g} representation of D_{2h} , see table 1.3) the average of the order parameter over the Fermi surface will, in general, be non-zero, and hence T_c is not suppressed [97]. However, for order parameters which transform under the operations of the point group like any representation other

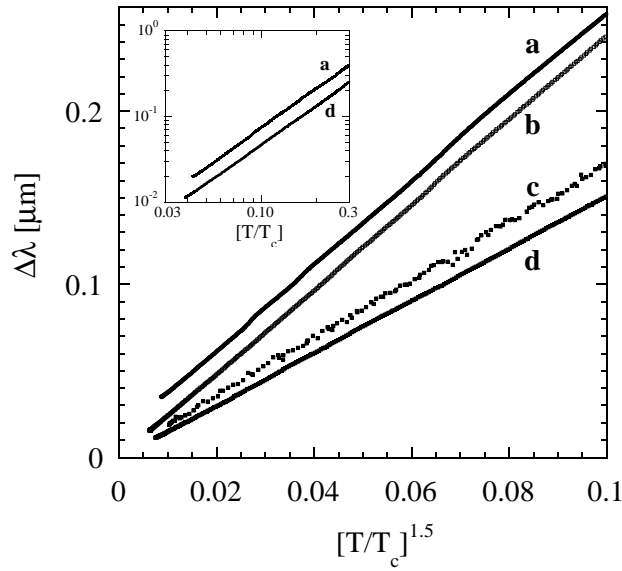


Fig. 1.5. Experimental evidence for unconventional superconductivity in half-filled quasi-two-dimensional organic charge transfer salts from the temperature dependence of the penetration depth (relative to the penetration depth extrapolated to $T = 0$). The data is taken from [95]. Samples a and b are κ -(ET) $_2$ Cu[N(CN) $_2$]Br, while samples c and d are κ -(ET) $_2$ Cu(NCS) $_2$ (note that the non-linear scale on the abscissa and that the data have been offset for clarity). The inset shows the data for samples a and d on a log scale. It is clear that $\Delta\lambda \sim (T/T_c)^{\frac{3}{2}}$. For an ‘s-wave’ gap (transforming like the identity representation) one expects $\Delta\lambda \sim \exp(-k_B T/\Delta_0)$ at low temperatures whereas one expects a power law behaviour when there are nodes in the gap. However, there remains an unexplained feature in this data: the power law is not what is expected in simple theories where one expects $\Delta\lambda$ to vary either linearly or quadratically with temperature at low temperatures. Experiments such as this and that in figure 1.4 suggest that the pairing state of the organic charge transfer salts has a lower symmetry than the crystal. In particular we argue in section 1.5 that orthorhombic materials, such as κ -(ET) $_2$ Cu[N(CN) $_2$]Br, have order parameters which transform like the B_{2g} representation of D_{2h} and so may be termed ‘ $d_{x^2-y^2}$ ’ superconductors. We also argue that monoclinic materials, such as κ -(ET) $_2$ Cu(NCS) $_2$, have order parameters which transform like the B_g representation of C_{2h} and so they may be termed ‘d-wave’ superconductors.

than the trivial representation, that is for all ‘non-s-wave’ states, the average of the order parameter over the Fermi surface must vanish by symmetry. Therefore, it can be shown [100,101] that non-magnetic disorder suppresses the critical temperature of unconventional superconductors according to the Abrikosov-Gorkov [102] formula,

$$\ln\left(\frac{T_{c0}}{T_c}\right) = \psi\left(\frac{1}{2} + \frac{\hbar}{4\pi k_B T_c \tau}\right) - \psi\left(\frac{1}{2}\right), \quad (1.10)$$

where T_{c0} is the superconducting critical temperature in the pure system, $\psi(x)$ is the digamma function and τ is the quasiparticle lifetime due to scattering from impurities. It was recently pointed out that a large number of experiments in the literature show that in the organic charge transfer salts presumably non-magnetic impurities suppress T_c in just the way predicted by the Abrikosov-Gorkov formula [96]. This has led to new experiments specifically designed to investigate the role of disorder in organic charge transfer salts [43]. These experiments have, however, not conclusively resolved the pairing symmetry. Indeed these experiments have resulted in a new puzzle. Analytis *et al.* [43] irradiated samples of κ -(ET)₂Cu(NCS)₂ with both protons and x-rays (both leading to similar results). Fig 1.4 shows the observed critical temperature plotted against the residual resistivity of the sample. While this initially follows the Abrikosov-Gorkov curve, for larger irradiation doses, the suppression of T_c is weaker than predicted. While this behaviour seems rather inconsistent with a pure ‘s-wave’ order parameter a detailed explanation of this phenomena is lacking.

The vortex lattice in the Abrikosov phase can yield important information about the pairing symmetry. In particular for an isotropic order parameter one expects a triangular vortex lattice [103, 104]. While, for an anisotropic order parameter either a square or a triangular lattice may occur as the energy difference between the square and triangular vortex lattices is less than 1% even for an isotropic order parameter [103, 104]. In particular square vortex lattices are found in Sr₂RuO₄, UPt₃ and YBa₂Cu₃O_{7-x} [104], all of which are believed to be unconventional superconductors. In the organic charge transfer salts a triangular lattice is observed [105] by muon spin relaxation (μ SR) experiments, which does not give a strong indication of what the pairing symmetry is.

We believe that a ‘ $d_{x^2-y^2}$ ’ order parameter transforming as the B_{2g} representation of D_{2h} in the orthorhombic materials and a ‘d-wave’ order parameter transforming as the B_g representation of C_{2h} in the monoclinic crystals [24] is most consistent with currently available data. However, there is no clear ‘smoking gun’ experiment supporting this conclusion. We eagerly await such an experiment and in the next section we review some of the further experiments that could be used to probe the pairing symmetry.

1.5.2 Possible probes of the pairing symmetry

We will now briefly discuss potential experiments that might provide an unambiguous determination of the pairing symmetry. Particular attention should be paid to directional probes such as ultrasonic attenuation, thermal conductivity and experiments on single crystals in a magnetic field. Directional probes have yielded important information about the gap structure in the

cuprates [98], UPt_3 [106] and Sr_2RuO_4 [107], so we will review what has been learnt by such methods these materials.

Effect of an orientated magnetic field in the conducting plane on the heat capacity, nuclear spin lattice relaxation rate, penetration depth and interlayer resistance

In the vortex state of a superconductor with nodes in the energy gap it can be shown that one effect of the applied magnetic field is to introduce a Doppler shift to the quasiparticle energy due to circulating supercurrents [108, 109]. Using this semiclassical theory Vekhter *et al.* [110] showed that in a ‘ $d_{x^2-y^2}$ ’ superconductor with a circular Fermi surface the density of states at the Fermi level, $D(E_F, \alpha)$, where α is the angle between the field and the antinodal direction, has a four fold variation as a magnetic field is rotated around the highly conducting plane. $D(E_F, \alpha)$ is maximal when \mathbf{H} is aligned in the antinodal direction and minimal for \mathbf{H} parallel to the nodes.

The variation in $D(E_F, \alpha)$ should be directly reflected in the behaviour of the electronic contribution to the specific heat $C_v(\alpha)$ which is predicted [110] to show a four-fold variation as \mathbf{H} is rotated around the highly conducting plane. Further Vekhter *et al.* predict that $C_v/T \propto \sqrt{HT}$ for the field in the nodal direction and that $C_v/T \propto \sqrt{HT^2}$ for the field in the antinodal direction. Similar effects are predicted for the $\mathbf{H}(\alpha)$ dependence of the nuclear lattice relaxation rate $1/T_1T$, the penetration depth λ [110] and the interlayer resistance [111].

Vekhter *et al.* also discuss the effect of lowering the symmetry of the unit cell and thus introducing a small ‘s-wave’ admixture to the order parameter. They show that even a very small ‘s-wave’ component reduces the four-fold variation of $D(E_F, \alpha)$ to a two-fold variation. However, experimentally great care would be required to detect a two-fold variation in, for example, C_v as any slight mismanagement of the field out of the plane would cause a similar two-fold variation because of the anisotropy between $H_{c2\parallel}$ and $H_{c2\perp}$, where $H_{c2\parallel}$ is the in plane upper critical field and $H_{c2\perp}$ is the out of plane upper critical field [112].

Deguchi *et al.* [112] have observed four-fold variation in $C_v(\alpha)$ in Sr_2RuO_4 . However, they interpret this as evidence of an anisotropic (but nodeless) gap on the γ sheet of the Fermi surface. In fact Deguchi *et al.* observed two different four-fold observations as a function of the applied magnetic field strength. For $|\mathbf{H}| \lesssim H_{c2\parallel}$ they observe an oscillation which they attribute to the anisotropy of $H_{c2\parallel}$ in the basal plane of Sr_2RuO_4 . At intermediate fields there are no oscillations in $C_v(\alpha)$ and for $H_{c1} < |\mathbf{H}| \ll H_{c2\parallel}$ Deguchi *et al.* observe oscillations in $C_v(\alpha)$ that are $\pi/4$ out of phase with those in the high field region. It is these low field oscillations that appear to associated with the anisotropy of the superconducting gap. In the organic charge transfer salts the in plane upper critical field is Clogston–Chandrasekhar (or Pauli) limited, [87] and there is therefore no anisotropy in $H_{c2\parallel}(\alpha)$ so one should not expect the

four-fold oscillations in the high field region because of variations in $H_{c2\parallel}(\alpha)$. However, this observation does indicate the ease with which extraneous effects can enter this type of experiment and therefore the care with which any such data needs to be interpreted.

Two related predictions are that for a gap with line nodes that $C_v \sim H^{\frac{1}{2}}T$ for $H \neq 0$ and $T \ll T_c$ in a polycrystalline sample [108, 113] and also that the heat capacity scales [114] as a function of $H^{\frac{1}{2}}T$. Both of these predictions have been confirmed for $\text{YBa}_2\text{Cu}_3\text{O}_{7-x}$ [115] and $\text{La}_{2-x}\text{Sr}_x\text{CuO}_4$ [116].

None of the effects described in this section appear to have been studied systematically in any of the organic charge transfer salts. Clearly such experiments could be extremely powerful tools for elucidating the structure of the gap in the organic charge transfer salts.

Thermal conductivity

In the cuprates, UPt_3 and Sr_2RuO_4 the thermal conductivity is dominated by quasiparticles (rather than phonons) over a significant temperature range below T_c . When quasiparticles dominate the measurements the dependence of thermal conductivity of a type II superconductor in the Abrikosov phase on the orientation of the magnetic field can yield information about the structure of the superconducting order parameter. For a superconductor with an isotropic gap one expects that the thermal conductivity, κ varies as $\cos\theta$ where θ is the angle between the heat current and the magnetic field [117]. This prediction has been confirmed in Nb [118]. With a thermal gradient along the a - [53] or b -axes [119] of $\text{YBa}_2\text{Cu}_3\text{O}_{7-x}$ an additional four fold variation in $\kappa(\theta)$ is observed when a magnetic field is rotated in the basal plane. The thermal conductivity is maximal at $\theta = \pi/4 + n\pi/2$ for $n \in \mathbb{Z}$ and therefore consistent with ‘ $d_{x^2-y^2}$ ’ superconductivity, i.e., the thermal conductivity is maximal with the field aligned in the antinodal direction [120]. In contrast in the (low temperature, low field) B phase of UPt_3 only the two fold variation of $\kappa(\theta)$ expected for an isotropic gap is observed when the field is rotated in the basal plane [121]. This is consistent with either an E_{2u} or an E_{1g} hybrid gap structure [106].

In Sr_2RuO_4 a four fold anisotropy is observed in $\kappa(\theta)$ as the field is rotated in the basal plane [122]. However, this is believed to be a result of the tetragonal crystal structure rather than a reflection of nodes (or anisotropies) in the gap [107]. In particular in Sr_2RuO_4 the fourfold anisotropy is a much weaker than the effect in $\text{YBa}_2\text{Cu}_3\text{O}_{7-x}$, and 20 times smaller than that predicted [123] for a gap with vertical line nodes.

Izawa *et al.* have measured the thermal conductivity of κ -(ET) $_2\text{Cu}(\text{NCS})_2$ as a magnetic field is rotated in the conducting (b - c) plane [93]. They observe a small (0.2% for $T < 0.6$ K) fourfold variation in $\kappa(\theta)$. This fourfold anisotropy has its maximum when the field is at 45° to the b and c axes (i.e., along the x and y axes as defined in figure 1.1). Therefore, Izawa *et al.* propose that

the superconducting order parameter of κ -(ET)₂Cu(NCS)₂ has ‘ d_{xy} ’ symmetry. However, one should be cautious of this interpretation because a ‘ d_{xy} ’ order parameter transforms like the A_g representation of C_{2h} (see table 1.4). Therefore, the anisotropy Izawa *et al.* observe is has the *same* symmetry as the lattice. Therefore, the observed anisotropy is compatible with variations caused by the crystal lattice itself and the observed effect is rather small. Indeed Izawa *et al.* also observed a large twofold anisotropy, which they claim is “mainly due to phonons”.

Furthermore, Izawa *et al.*’s interpretation is based on the assumption that there is strong interlayer coupling, which may not correct for κ -(ET)₂Cu(NCS)₂. In particular the theory used to interpret these experiments requires that the superconductivity may be described by a (highly anisotropic) three dimensional Ginzburg-Landau theory. However, in κ -(ET)₂Cu(NCS)₂ there is a very real possibility that the layers are Josephson coupled; in which case a three dimensional Ginzburg-Landau theory could not be applied to these results. In particular Izawa *et al.*’s interpretation of the data requires that vortices are formed when the field is parallel to the highly conducting layer.

The thermal conductivity of λ -(BETS)₂GaCl₄ and κ -(BETS)₂FeBr₄ has also been measured by Tanatar and co-workers [124]. However, in this work the field was not rotated in the conducting plane, so we will not discuss it further.

Ultrasonic attenuation

Because the velocity of sound is much less than the velocity of an electron at the Fermi surface ($v_s \ll v_F$), longitudinally polarised ultrasound is only attenuated effectively by electrons moving almost perpendicular to the direction of sound propagation [125]. This makes longitudinal ultrasound a powerful probe of the anisotropy of the superconducting gap, indeed longitudinal ultrasonic attenuation experiments were among the first to probe gap anisotropy in conventional superconductors such as Sn [80]. Transverse ultrasound experiments are extremely sensitive to gap anisotropies as the attenuation depends on both the direction of sound propagation and the direction of the polarisation.¹¹ Such experiments have been important for determining the gap structure of both UPt₃ [126, 127] and Sr₂RuO₄ [128].

Measurements of attenuation of longitudinal ultrasound perpendicular to the highly conducting planes have been made in κ -(ET)₂Cu(NCS)₂ [59, 129, 130], κ -(ET)₂Cu[N(CN)₂]Br [59, 131] and κ -(ET)₂Cu[N(CN)₂]Cl [60]. A clear coupling to the electronic degrees of freedom is seen as the crossover from the ‘bad-metal’ to the Fermi liquid is observed at temperatures corresponding to the maximum in the resistivity. Indeed the electronic pressure-temperature

¹¹For a clear explanation of this phenomena see [107] and [126] and references therein.

phase diagram of κ -(ET)₂Cu[N(CN)₂]Cl has been mapped out using ultrasound [60]. However, none of these experiments were designed to measure the anisotropy of the superconducting order parameter.

Ultrasound experiments are complicated by the small size and the shape of single crystals of organic charge transfer salts [59, 130]. However, for example, the crystal of κ -(ET)₂Cu(NCS)₂ studied by Simizu *et al.* [130] (which was reported to be $1.35 \times 5.06 \times 1.62$ mm³) is rather similar size and shape to the crystal of UPt₃ studied by Ellman *et al.* [126] ($1 \times 1 \times 2.7$ mm³). Therefore, there does not seem to be any intrinsic reason why transverse ultrasound could not be used to study the order parameter of organic superconductors. Given the importance of such experiments [80, 126–128] in UPt₃, Sr₂RuO₄ and Sn transverse ultrasound appear to be an excellent tool to probe the structure of the gap in organic charge transfer salts.

1.5.3 Superfluid stiffness (evidence for a non-BCS groundstate and pairing mechanism)

The defining property of a superconductor is the Meissner effect, i.e., perfect diamagnetism [104]. The strength of the Meissner effect is measured by the superfluid stiffness, $D_s \equiv c^2/4\pi\lambda^2$, where λ is the penetration depth, as the superfluid stiffness is the constant of proportionality between the vector potential of an applied magnetic field and the induced supercurrent. Thus the smaller the superfluid stiffness the ‘weaker’ the superconductivity. In the underdoped cuprates it is found that $T_c \propto D_s$: this is the Uemura relation [132].

A number of exotic mechanisms have been proposed to explain the Uemura relation and it is natural in both the preformed pairs scenario [133] and the resonating valence bond (RVB) theory [134]. However, the Uemura relation in the underdoped cuprates is even predicted within BCS theory [135]. In BCS theory $D_s \propto n_s/m^*$, where n_s is the density of electrons in the superfluid condensate. However, we stress that there is no way to directly measure n_s and, in general, n_s is not required to be the same as the electron density, n , even at $T = 0$ (for example only about 10% of the atoms form the condensate in ⁴He at absolute zero [136, 137]). However, BCS theory is a weak coupling theory and $n_s = n$ at $T = 0$. Recall that the doping, x , is an implicit parameter when one compares T_c and D_s in the underdoped cuprates. Therefore, the Uemura relation can be derived from BCS theory by noting that $T_c \sim x$, which is observed experimentally for small x , and that $D_s \propto n_s = n \propto x$ which assumes m^* is independent of, or only weakly dependent on, doping.

Pratt and coworkers [138] have systematically measured the critical temperatures and penetration depths of a large number of organic charge transfer salts. This data, along with that of several other groups [139, 140] is shown in figure 1.6. It is important realise that the implicit parameters in this plot are chemical substitution and pressure, which do not change the filling factor: all of these materials are half-filled [141]. The role of pressure, be it ‘chemical’

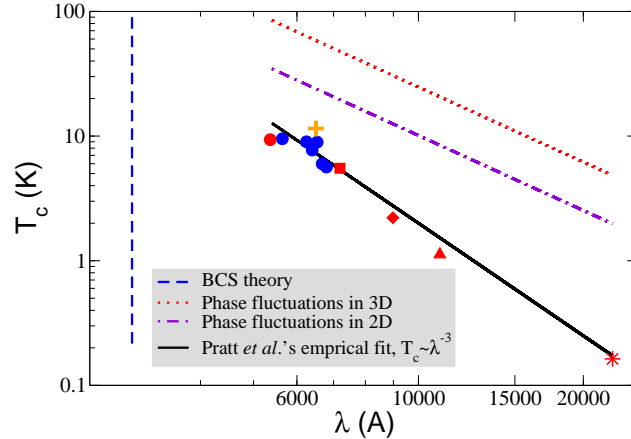


Fig. 1.6. The small superfluid stiffness observed in organic charge transfer salts with low critical temperatures provides clear evidence that the superconductivity is not described by BCS theory. The predictions of the phase fluctuation theory proposed for the cuprates by Emery and Kivelson [133] is also to overestimate the critical temperature. This data is extremely surprising as the data on the left corresponds to materials where the interactions are stronger, e.g., the effect mass is larger [141]. Thus the superfluid stiffness $D_s \propto 1/\lambda^2$, where λ is the zero temperature penetration depth, gets smaller (and hence less like the BCS prediction) as we move away from the Mott transition. This is unexpected as the spectral weight in the quasiparticle peak increases as the correlations become weaker, so we might expect the superfluid stiffness to be smallest near the Mott transition [30, 142]. Note that all of these materials are half-filled [141] so doping effects cannot be invoked to explain the data. This figure is modified from [141], while the data is from Pratt *et al.* [138], Lang *et al.* [139] and Larkin *et al.* [140] (colour of citation matches colour of data points). The figure shows data for κ -ET₂Cu[N(CN)₂]Br (+), κ -ET₂Cu(NCS)₂ at several pressures (●), λ -BETS₂GaCl₄ (■), β -ET₂IBr₂ (◆) α -ET₂NH₄Hg(NCS)₄ (▲) and κ -BETS₂GaCl₄ (★).

or hydrostatic, in these materials is to drive them away from the Mott transition [28]. Generically, it is also found that increasing the pressure lowers T_c . Therefore, the data points on the left hand side of figure 1.6 are closer to the Mott transition than those on the right hand side.

As there is no doping of the system BCS theory (and other weak coupling theories) does not predict any change in n_s as pressure varies T_c (whence the vertical line in figure 1.6). However, one might object that as we lower pressure and drive towards the Mott transition m^* increases. If one includes this effect the prediction is that the superfluid stiffness is smallest closest to the Mott transition. This is the *opposite* behaviour to that seen experimentally. It seems extremely unlikely that using Eliashberg theory to account for strong coupling phononic effects will rectify this essential disagreement with experiment [141]. Therefore, Pratt *et al.*'s data [138] provides the clearest evidence (i) for a

non-phononic pairing mechanism and (ii) that weakly correlated theories are insufficient to explain the observed superconductivity in the organic charge transfer salts [141].

1.6 Strongly correlated models of superconductivity: frustration and RVB

Most of the early work on superconductivity in the organic charge transfer salts took weakly correlated approaches. A comprehensive review of this work was recently published by Kuroki [143], and, rather than duplicating that effort here, we limit ourselves to a few general comments. The two most studied weakly correlated theories of superconductivity in the organic charge transfer salts are the Eliashberg phononic pairing mechanism and the spin-fluctuation pairing mechanism [with calculations most often performed within the fluctuation-exchange (FLEX) approximation]. Neither of these approaches capture the Mott transition or the large effective mass enhancement seen in the organic charge transfer salts. Therefore, one must clearly go beyond a weakly correlated description of the superconductivity in order to provide a complete description of the full range of behaviours observed in the organic charge transfer salts (c.f. sections 1.3 and 1.4). Further, the small superfluid stiffness observed in the low T_c materials (figure 1.6 and section 1.5.3) cannot be accounted for within weakly correlated theories [141].

Recently a number of groups have proposed strongly correlated theories of the organic charge transfer salts. These are based on the Hubbard model described in section 1.2.2. A number different methods have been discussed [30, 144–149] with rather similar results. Here we focus on the simplest of these theories, the resonating valence bond (RVB) or gossamer superconductor theory (the two names have been used interchangeably in the literature).

The celebrated BCS wavefunction [4] is

$$|BCS\rangle = \prod_{\mathbf{k}} \left(u_{\mathbf{k}} + v_{\mathbf{k}} \hat{c}_{\mathbf{k}\uparrow}^\dagger \hat{c}_{-\mathbf{k}\downarrow}^\dagger \right) |0\rangle, \quad (1.11)$$

where $|0\rangle$ is the vacuum state and the $u_{\mathbf{k}}$ and the $v_{\mathbf{k}}$ are variational parameters. The RVB wavefunction is a projected BCS wavefunction,

$$|RVB\rangle = \hat{P}_G |BCS\rangle, \quad (1.12)$$

where

$$\hat{P}_G = \sum_i (1 - \alpha \hat{n}_{i\uparrow} \hat{n}_{i\downarrow}) \quad (1.13)$$

is the partial Gutzwiller projector. For $\alpha = 1$ the Gutzwiller projector removes all double occupation from the wavefunction. The $\alpha = 1$ RVB state has been

studied since the early days of high- T_c [10, 134]. However, as no double occupation can occur for $\alpha = 1$ this state is always insulating for half-filled systems and therefore will not give the correct description of the organic charge transfer salts. However, if we treat α as a variational parameter [150, 151] then some double occupation is allowed, and superconducting and metallic states may occur.

The simplest approach to this theory is to make the Gutzwiller approximation (as well as the Hartree-Fock-Gorkov approximation implicit in the BCS state) in which one enforces the constraints on the fraction of doubly occupied sites only on average. This allows one to derive a strongly correlated mean-field theory with only a few parameters [150, 151]. Studies of this theory [30, 144, 146] have shown that the superconducting state: (i) undergoes a first-order Mott transition as is seen experimentally (in the mean-field theory this is of the Brinkman-Rice type [152]); (ii) has quasiparticles with a large effective masses which are strongly enhanced near the Mott transition as is seen in experiments; and (iii) has a strongly suppressed superfluid stiffness. The RVB theory also predicts that there is a pseudogap above the superconducting state in agreement with NMR experiments (see section 1.8.2). Furthermore, it has already been shown that the insulating state of the RVB theory supports both Néel ordered states [146, 148, 149] like that observed in the insulating state of κ -(ET)₂Cu[N(CN)₂]Cl and spin-liquid states [30, 145, 149] like those observed in the insulating state of κ -(ET)₂Cu₂(CN)₃ and β' -[Pd(dmit)₂]₂Z (see section 1.8.5). However, to date there has been relatively little work [149] on the comparative stability of these states as the frustration is varied. Another important task for these theories yet to be reported is to give a detailed explanation of the small superfluid stiffness seen in the low- T_c materials (see figure 1.6 and section 1.5.3).

1.7 The phase diagram of the Hubbard model on the anisotropic triangular lattice

Eight years ago [25] one of us proposed a speculative zero temperature phase diagram for the Hubbard model on an anisotropic triangular lattice. We now know significantly more about the phase diagram because there have been many studies of this model utilising many different approximation schemes and numerical techniques. In figure 1.7 we sketch a schematic phase diagram which summarises current knowledge.

1.7.1 The Mott transition

Only a few points on the phase diagram are known exactly. Because of perfect nesting the Mott metal-insulator transition occurs at an infinitesimal U for both the square lattice ($t' = 0$) and isolated 1D chains ($t = 0$) [153]. For the isotropic triangular (or more correctly, hexagonal) lattice ($t' = t$) there is no

nesting at half filling and so the Mott transition occurs at a finite U . The critical U has been estimated by a variety of methods [11, 30, 154, 155] and seems to be about $U = 10t - 15t$. We therefore sketch the Mott transition as passing smoothly between these three points in our phase diagram. Several approximations suggest that the Mott transition is first order throughout the (zero temperature) phase diagram, however the recent work of Imada *et al.* [71, 72] and the critical exponents measured by Kawagwa *et al.* [70] has called this into question. In particular Imada *et al.* propose that for some frustrations the transition is first order while for others there is a (marginal) quantum critical point. All of the other phase transitions shown in the schematic phase diagram (figure 1.7) are thought to be second order.

1.7.2 The superconducting states

A number of studies based on strongly correlated theories [30, 144–146, 148, 149] suggest that superconductivity is realised on the metallic side of the Mott transition. This superconductivity is mediated by antiferromagnetic interactions which occur because of superexchange. As the superexchange interactions are only relevant in the large U limit, for small U this interaction will vanish and so will the superconductivity, leaving a metallic state for $W \gg U$.

The symmetry of the anisotropic triangular lattice is represented by the C_{2v} point group, which is summarised in table 1.5. Various calculation methods indicate that in the small t'/t limit the superconducting order parameter transforms like the A_2 representation of C_{2v} [24, 144]. This is colloquially referred to as ‘ $d_{x^2-y^2}$ ’ superconductivity (see section 1.5.1 for a discussion of this nomenclature). FLEX [143] and weak-coupling renormalisation-group [167] studies also predict that the superconducting state has this symmetry. However, for $t = t'$ the model has C_{6v} symmetry. Here ‘ $d_{x^2-y^2}$ ’ state belongs to the two-dimensional E_2 representation. This has recently led to the proposal that for $t \sim t'$ a ‘ $d + id$ ’ state (which is a mixed state transforming like a complex combination of both the A_1 and A_2 representations of C_{2v}) is realised [24, 144]. These arguments also suggest that in the large t'/t limit the state transforming like the A_1 representation of C_{2v} , which may be colloquially referred to as a ‘ $d_{xy} + s$ ’ state, occurs [24, 144]. We therefore sketch these different superconducting states in figure 1.7.

1.7.3 The insulating states

We now turn our attention to the insulating state. We begin by considering the large U/W limit, in which our Hubbard model reduces to the Heisenberg model on the anisotropic triangular lattice. This model contains two parameters, $J = 4t^2/U$ and $J' = 4t'^2/U$ which occur because of superexchange: a second order perturbation effect. All higher order processes can be neglected because we are in the large U limit. For small J'/J it is well established that the Néel state is realised. Series expansions [156] show that the Néel state is

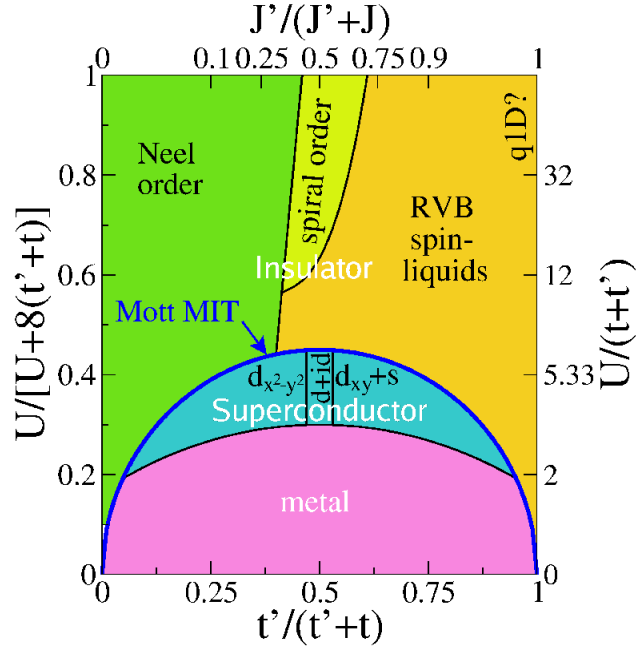


Fig. 1.7. Schematic diagram of the proposed zero temperature phase diagram of the Hubbard model on the anisotropic triangular lattice at half filling. We argue throughout this review that this model provides a qualitative description of the β , β' , κ and λ phase organic charge transfer salts. The central feature of the phase diagram is the Mott transition. We have argued that superconductivity occurs on the metallic side of the Mott transition. It has been proposed that the symmetry of the superconducting state varies as the frustration is varied and that the superconducting state breaks time reversal symmetry when the lattice is approximately hexagonal ($t \sim t'$) [24, 144]. We label the superconducting states by their symmetries (the colloquial names are given a more formal basis in table 1.5). It should be stressed that the proposed superconducting states are strongly correlated and RVB like rather than weakly correlated BCS states [30, 144–146, 148, 149]. As the correlations, which mediate the superconductivity, are reduced we recover a metallic groundstate. For $U \gg t, t'$ the Hubbard model at half filling is insulating and the spin degrees of freedom can be described by the Heisenberg model. On the basis of the calculations reported in [156–160] we have also argued that the insulating states should change from Néel order to spiral ordered states to a spin-liquid as t'/t is increased, i.e., as the frustration is varied. Near the Mott transition corrections to the Heisenberg model, such as ring exchange are important. This may stabilise the spin-liquid [161]. This phase diagram includes all of the phases observed in the layered organic charge transfer salts at low temperatures. We have shown elsewhere in this review (particularly sections 1.3, 1.4 and 1.6) that the finite temperature behaviour of the half-filled layered organic charge transfer salts is also described by the Hubbard model on an anisotropic triangular lattice. Hence we conclude that that the Hubbard model on the anisotropic triangular lattice provides an excellent qualitative description of these materials.

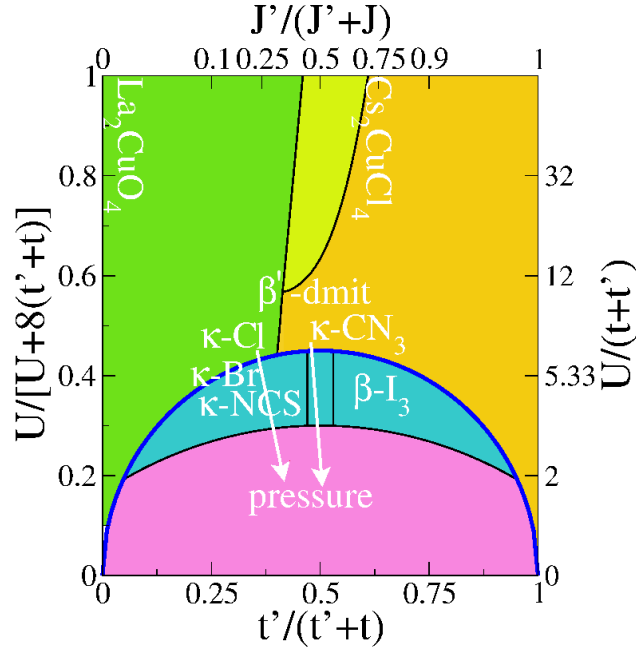


Fig. 1.8. The same phase diagram as is shown in figure 1.7 with the labels removed (for clarity) and the names of some materials added. The position of name indicates our guesstimate of where that material sits on the proposed phase diagram, the white arrows indicate the proposed effect of pressure. This is very rough and accurately determining the details of the parameter values corresponding to specific materials at particular pressures is a major challenge (see in particular section 1.8.1). The following shorthand is used in the figure: κ -Cl is κ -(ET)₂Cu[N(CN)₂]Cl, κ -CN₃ is κ -(ET)₂Cu₂(CN)₃, κ -Br is κ -(ET)₂Cu[N(CN)₂]Br, κ -NCS is κ -(ET)₂Cu(NCS)₂, β -I₃ is β -(ET)₂I₃ and β' -dmit is β' -[Pd(dmit)₂]₂Z. La₂CuO₂, the parent compound of the cuprates, is shown with a large U and on the square lattice ($t' = 0$) to emphasise the similarities between the organics and the cuprates [162]. It is known experimentally that $J'/J \approx 3$ in Cs₂CuCl₄ [163]. Cs₂CuCl₄ has a spirally ordered ground state at very low temperatures, but shows a region of spin-liquid like behaviour at higher temperatures [164] which may indicate that the spin-liquid state is energetically close to the ground state and that coupling in the third dimension plays an important role in the real material. κ -(ET)₂Cu₂(CN)₃ shows a spin-liquid ground state [165], while the β' -[Pd(dmit)₂]₂Z salts seem to be on the boarder between magnetic ordering and spin-liquid behaviour. The nature of this magnetic ordering is not yet clear. Pressure drives κ -(ET)₂Cu[N(CN)₂]Cl from a the Néel state via the superconducting state to normal metal. While κ -(ET)₂Cu[N(CN)₂]Br is so close to the Mott transition that it can be driven insulating by deuteration of the ET molecule. Huckel calculations suggest that β -(ET)₂I₃ (and other β phase salts) have $t' > t$ [166]. If our speculative phase diagram is correct then this suggests that they have a different pairing symmetry to the κ -phase materials [24, 144]. This also suggests that the superconducting states of κ -(ET)₂Cu₂(CN)₃ and β' -[Pd(dmit)₂]₂Z may break time reversal symmetry [24, 144].

Irrep	E	C_2	σ^+	σ^-	Required nodes	Example basis functions	Colloquial names
A_1	1	1	1	1	none	$1_{\mathbf{k}}, X_{\mathbf{k}}Y_{\mathbf{k}}$	$s, d_{xy}, s + d_{xy}$
A_2	1	1	-1	-1	line	$X_{\mathbf{k}}^2 - Y_{\mathbf{k}}^2$	$d_{x^2-y^2}$
B_1	1	-1	1	-1	line	$X_{\mathbf{k}} + Y_{\mathbf{k}}$	p_{x+y}
B_2	1	-1	-1	1	line	$X_{\mathbf{k}} - Y_{\mathbf{k}}$	p_{x-y}

Table 1.5. The character table, symmetry required nodes and some basis functions of the irreducible representations of the point group C_{2v} . C_{2v} represents the symmetry of the anisotropic triangular lattice. The functions $1_{\mathbf{k}}$, $X_{\mathbf{k}}$ and $Y_{\mathbf{k}}$ may be any functions which transform, respectively, as 1, k_x and k_y under the operations of the group and satisfy translational symmetry. The operations in the group are the identity, E , rotation about the z -axis by π , C_2 , and reflection through the planes $k_x = \pm k_y$, σ^\pm . A brief explanation of characters is given in the caption to table 1.3. Note that inversion symmetry is not an operation of the group. This might suggest that singlet and triplet states are not differentiated by symmetry. However, as we are discussing the symmetry of a two dimensional lattice, rotation by π (which is an operation in the group) differentiates between singlet and triplet states.

stable for $J'/J < 0.7$. For $J = 0$ we have uncoupled one-dimensional chains along the diagonal on the unit cell. The Heisenberg model can be solved exactly in one-dimension and the ground state is a spin-liquid with deconfined spinon excitations [168]. The question of what happens when there is a finite coupling to a second dimension (finite J) is extremely subtle. However, recent work [147, 156, 169] suggests that this physics does survive to a significant degree in frustrated systems and that a spin-liquid occurs in some parts of the phase diagram with $J' > J$. Therefore, we label the large J'/J region of the phase diagram ‘q1D?’.

Various theoretical studies of the Heisenberg model on the anisotropic triangular lattice have been performed. The methods used include linear spin wave theory [157] and large- N mean field theory [158]. Both of these methods indicate that when frustration destroys Néel order [which has the ordering wavevector $\mathbf{q} = (\pi, \pi)$] a spiral state [with ordering wavevector $\mathbf{q} = (q, q)$] occurs. In the spiral state q varies from π , at the critical frustration where the Néel state gives way to spiral order, to $\pi/2$ at large frustration which is the classical value for uncoupled chains. At $J' = J$ these theories give $q = 3\pi/2$ which describes the ‘classical 120°-state’: the classical solution of the isotropic triangular lattice [159]. In the classical 120°-state the spins on neighbouring sites align at an angle 120° apart from their nearest neighbours. It is widely believed that the quantum analogue of ‘120°-state’ is the true ground state of the Heisenberg model on the isotropic triangular lattice [156, 160]. By analogy it may be argued that quantum-spiral states are the ground states of the Heisenberg model on the anisotropic triangular lattice in the regime $J' \sim J$. This is certainly what is suggested by the large- N studies [158]. However, it is not yet clear how or at what parameter values the spiral state changes into the spin-liquid.

At lower values of U/W (i.e., near the Mott transition) higher order perturbation processes cannot be neglected. For example, ring exchange processes (which is of order t^4/U^3) [161] and hopping around triangular clusters (which is of order t^2t'/U^2) [11] may become important. Both of these processes favour RVB spin-liquid states. This may explain the observation of a spin-liquid state in insulating phase of κ -(ET)₂Cu₂(CN)₃ [165] and β' -[Pd(dmit)₂]₂Z [170] (see section 1.8.5). Therefore, we add an RVB spin-liquid phase to our sketch of the phase diagram intervening between the quasi-one-dimensional phase and the spiral order. We also include the enhancement of the region of stability of this phase near to the Mott transition.

1.8 Some outstanding problems

Before drawing our conclusions, we briefly indulge ourselves by discussing what we see as some of the major problems in the field that we have not discussed significantly above.

1.8.1 Deducing parameters for the minimal models from first principles electronic structure calculations

We have argued above that the physics of the organic charge transfer salts can be understood in terms of the Hubbard model on the anisotropic triangular lattice. Clearly it is vitally important, for this program, to know accurately what values of the parameters of this model (t , t' and U) correspond to a given material at a given pressure. Understandably, given the chemical complexity and large unit cells of the organic charge transfer salts, most theoretical work on the band structure of these materials has used the Huckel model [15]. (There has also been considerable effort expended to determine the values of t and t' experimentally [171].) However, recent advances in computational speed and the computational efficiency of electronic structure codes [172] have allowed the first density functional theory (DFT) studies of the band structures of organic charge transfer salts to be performed [17–20]. The calculations are significantly more accurate than the Huckel calculations and there is a great need for systematic studies of the band structures of a range organic charge transfer salts. In particular a detailed mapping from the experimental parameters of ‘chemical’ and hydrostatic pressure to the theoretical parameters of t and t' would enormously benefit the field. Further, this would greatly improve our ability to perform quantitative tests of theories of the Hubbard model in the organic charge transfer salts.

To complete the mapping between the experimental and theoretical parameters we also need to know how the dimer U varies with ‘chemical’ and hydrostatic pressure. This is a much more difficult task. To date the most common approach has been to estimate U from the intra-dimer hopping integral. We have shown in section 1.2.2, that this is not only inaccurate (as it is based

on extend Huckel calculations) but also incorrect as correlation effects, not the intra-dimer hopping integrals, determine the dimer U . Therefore, more accurate calculations are required. The ‘bare’ Hubbard- U of a dimer *in vacuo* can be straightforwardly determined from DFT as it is the second derivative of energy with respect to charge ($U = d^2E/dq^2$). However, in a crystal the effective Hubbard- U is greatly decreased as the second derivative of energy with respect to charge contains a large contribution due to the polarisability of the crystal. The problem of calculating the reduction in the Hubbard- U due to the polarisability of the molecules is simply a self-consistent problem in classical electrodynamics. This approach has been successfully applied to alkali doped fullerenes [47, 173]. Thus the large size and low electron density of molecular crystals is a singular advantage when it comes to calculating the Hubbard- U . Indeed this is such an advantage that, we believe, this makes molecular crystals an ideal class of materials in which to study first principles approaches to strongly correlated effects. We believe that the time is now ripe to apply this method to the organic charge transfer salts and thus to map from ‘chemical’ and hydrostatic pressure to the Hubbard- U .

If both of these procedures were accurately carried out then we would have a direct mapping between the Hubbard model and experiment. This would allow very direct testing of the hypothesis that the Hubbard model provides the correct microscopic description of the organic charge transfer salts. It would also allow for the experimental testing of the various approximations used to study the Hubbard model. Therefore, this mapping would not only be extremely important to the community interested in the organic charge transfer salts for their own sake, but would make the organic charge transfer salts an even more important test-bed for theories of strongly correlated quantum many-body systems than they are already. In figure 1.8 we sketch our best guess of which parameters correspond to which materials, based on the calculations performed thus far and comparison of the observed behaviour of these materials with figure 1.7. Given the comments above this is clearly a very rough procedure.

1.8.2 Is there a pseudogap?

NMR experiments on the organic charge transfer salts show a large decrease in the spin lattice relaxation rate, $1/T_1T$, the Knight shift, K_s , and the Korringa ratio, $1/T_1TK_s^2$ below about 50 K [83–85] (see figure 1.9). In this section we ask whether these experiments indicate the opening of a gap-like structure at the Fermi energy. The pseudogap phase in the cuprates has attracted a great deal of attention [174], yet there has been very little work on understanding the origin of these experimental effects in the organic charge transfer salts. Clearly a good starting point to investigate this effect in the organic charge transfer salts would be to follow a number of the experimental and theoretical approaches that have proved fruitful in investigating the pseudogap in the cuprates.

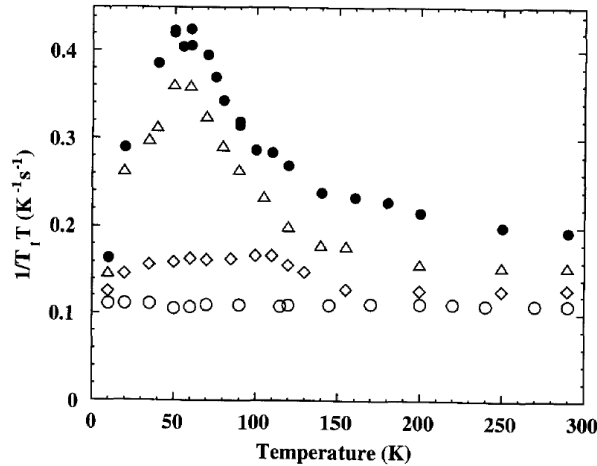


Fig. 1.9. Is the suppression of the nuclear spin relaxation rate, $1/T_1$, evidence for a pseudogap? This data (from [175]) shows the temperature dependence of $1/T_1T$ in κ -(ET)₂Cu[N(CN)₂]Br at various pressures [1 bar (●), 1.5 kbar (△), 3 kbar (◇) and 4 kbar (○)]. Rather similar effects are seen across a range layered organic charge transfer salts [85]. In materials that are close to the Mott transition a peak in $1/T_1T$ is observed in at around 50 K. This is not expected in weakly interacting systems. However, a pseudogap is predicted by the RVB theory of superconductivity [30] and appears to be a rather natural feature of extensions to dynamical mean field theory which include some spatial correlations [176,177]. A detailed theoretical understanding of this data is still lacking, as are further experiments probing the possibility that there is a pseudogap in the organic charge transfer salts.

One of the most important questions about the pseudogap in the cuprates has been whether, and if so how, it relates to superconductivity. The Nernst effect is much larger in a type-II superconductor than it is in a normal metal (because vortices carry entropy extremely efficiently). Therefore, the discovery of a large Nernst effect in the pseudogap regime [178] of the cuprates is suggestive of superconducting fluctuations playing an important role in the pseudogap [133]. In this context studies of the temperature dependence of the Nernst effect in materials which show the unexpected NMR behaviour {e.g., κ -(ET)₂Cu[N(CN)₂]Br and κ -(ET)₂Cu(NCS)₂} would be extremely interesting.

Theoretical avenues could also be productively pursued. In particular we need to discover the correct phenomenological description of the NMR data. The first question which needs to be addressed is can the NMR data be explained without invoking a gap in the density of states? For example, the maximum in $1/T_1T$ occurs at a temperature very close to that where the crossover from the ‘bad-metal’ to the Fermi liquid occurs. Could the origin of the maximum then be simply related to recovery of a Fermi-liquid Korringa-

like behaviour from the local moment (Heisenberg) physics associated with the ‘bad-metal’ [179–181] (charge fluctuations happen on significantly slower time-scales than spin fluctuations in the ‘bad-metal’)? Or, is a gap in the density of states necessary to describe the observed phenomena? A phenomenological description of the data will obviously provide clues to the appropriate microscopic description. Given the success of DMFT in describing many of properties of the organic charge transfer salts (see section 1.3.1), extensions to DMFT to include non-local effects seem an obvious avenue to explore [176]. Cellular DMFT (CDMFT) [176] and the dynamical cluster approximation (DCA) [176] are two such approaches. These approaches have already provided significant insights into the pseudogap in the cuprates, in particular the so-called Fermi arcs seen in angle resolved photoemission spectroscopy (ARPES) experiments [182,183] on the cuprates appear to be a natural feature in CDMFT [177]. Therefore, studies of the Hubbard model on an anisotropic triangular lattice within CDMFT or the DCA would be an extremely interesting approach.¹² It is interesting to note that many of the features present in the CDMFT description of the pseudogap are captured (in a somewhat cruder form) by the RVB theory (discussed in section 1.6). In particular the RVB theory predicts a pseudogap [30,144,146,151]. Therefore, a detailed understanding of the NMR experiments on the organic charge transfer salts will provide a stringent test of this theory.

1.8.3 Low T_c materials

Most of the attention to superconducting has been focused on materials with high transition temperatures and the region around the Mott transition. But, recently, the work Pratt, Blundell and coworkers [138,141,142] has shown the importance of materials with low critical temperatures for understanding superconductivity in the organic charge transfer salts (see figure 1.6 and section 1.5.3 for a discussion of this work). However, there remains very little data on the low- T_c materials. We believe that an extensive understanding of the phenomenology of these low- T_c materials is a vital prerequisite of a more detailed understanding of the superconducting states of *all* of the organic charge transfer salts. Therefore, there is a desperate need for more experimental and theoretical work on these materials.

1.8.4 Synthetic chemistry

It goes, almost, without saying that condensed matter physics cannot proceed without high quality samples. As such, synthetic chemistry plays the central role in the study of organic charge transfer salts, for, without it, the field could neither exist nor progress. Historically, much of the synthetic work in this

¹²One CDMFT study of the Hubbard model on an anisotropic triangular lattice has appeared in the literature but this problem was not addressed in that paper [149].

field has focused on discovering new organic charge transfer salts. However, we would like to stress the importance of the less obviously glamorous work of producing higher quality samples of materials which have already been extensively studied. As we have seen in this review there are many outstanding problems in the flavours of organic charge transfer salts that have been with us for the last twenty years. Many of these problems would be made significantly more tractable if new kinds of data were available. For example, a tricrystalline experiment, of the type so important in the cuprates [98], could lay to rest once and for all questions about the pairing symmetry in the organic charge transfer salts.

Perhaps the most pressing need for improvement in sample quality is size. Neutron scattering has been extremely important for our understanding of the cuprates [184], Na_xCoO_2 [11, 185] and many other strongly correlated materials. This is mostly because neutrons provide direct information about the spin degrees of freedom which are of vital importance in strongly correlated materials such as the organic charge transfer salts. Therefore, perhaps the single greatest impediment to the field is the lack of high quality single crystals for neutron studies. Taniguchi and coworkers have recently demonstrated that large single crystals can be grown [186] and one can only eagerly await the results of neutron scattering experiments on this sample and the growth of similarly large samples of other salts.

1.8.5 Do $\kappa\text{-(ET)}_2\text{Cu}_2(\text{CN})_3$ and/or $\beta'\text{-[Pd(dmit)}_2\text{]}_2\text{Z}$ have spin-liquid ground states?

A recent series of experiments on $\kappa\text{-(ET)}_2\text{Cu}_2(\text{CN})_3$ [165, 187] by Shimizu and coworkers has sparked considerable interest in the theoretical community [30, 56, 144, 145, 149, 161, 188–195]. This is because Shimizu *et al.* have gathered strong evidence that $\kappa\text{-(ET)}_2\text{Cu}_2(\text{CN})_3$ may have a spin-liquid ground state. A spin-liquid is a state in which there exist well formed local moments which do not magnetically order. Importantly a spin-liquid should possess *all* of the symmetries of the crystal. In a particularly beautiful demonstration of the spin-liquid behaviour in $\kappa\text{-(ET)}_2\text{Cu}_2(\text{CN})_3$ Shimizu *et al.* compared the spin susceptibility of $\kappa\text{-(ET)}_2\text{Cu}_2(\text{CN})_3$ with that of $\kappa\text{-(ET)}_2\text{Cu}[\text{N}(\text{CN})_2]\text{Cl}$ (see figure 1.10). Both $\kappa\text{-(ET)}_2\text{Cu}_2(\text{CN})_3$ and $\kappa\text{-(ET)}_2\text{Cu}[\text{N}(\text{CN})_2]\text{Cl}$ have well formed local moments with spin- $\frac{1}{2}$. In both systems the Heisenberg exchange interaction is about 250 K [25, 165]. However, the frustration is significantly larger in $\kappa\text{-(ET)}_2\text{Cu}_2(\text{CN})_3$ than it is in $\kappa\text{-(ET)}_2\text{Cu}[\text{N}(\text{CN})_2]\text{Cl}$ [56, 165, 196]. The susceptibility of $\kappa\text{-(ET)}_2\text{Cu}[\text{N}(\text{CN})_2]\text{Cl}$ diverges at ~ 25 K as the material undergoes the Néel transition. In contrast no magnetic transition is observed in $\kappa\text{-(ET)}_2\text{Cu}_2(\text{CN})_3$ down to 32 mK (the lowest temperature studied by Shimizu *et al.*).

Rather similar behaviour (also shown in figure 1.10) has been observed by Kato *et al.* [170] in a the series $\beta'\text{-[Pd(dmit)}_2\text{]}_2\text{Z}$, where Pd(dmit)_2 is the acceptor molecule 1,3-dithiol-2-thione-4,5-dithiolate (C_3S_5), $\text{Z}=\text{Me}_4\text{Y}$ or

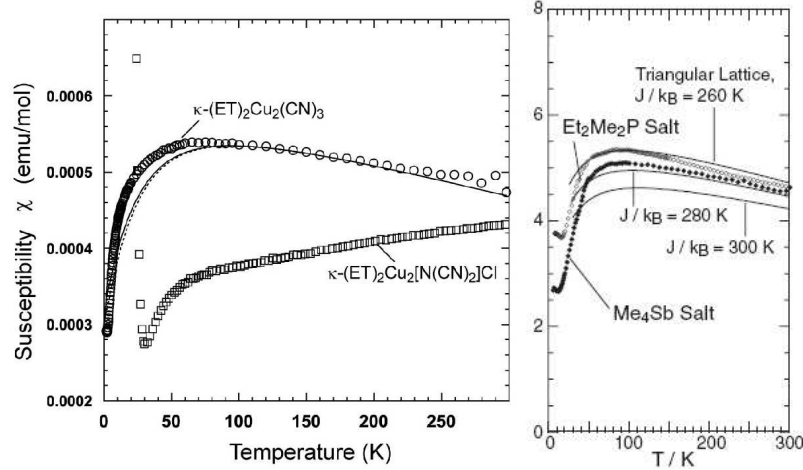


Fig. 1.10. Evidence for spin-liquid ground states in κ -(ET) $_2$ Cu $_2$ (CN) $_3$ and β' -[Pd(dmit) $_2$] $_2$ Z. The left panel (modified from [165]) compares the temperature dependencies of the magnetic susceptibilities, χ , of κ -(ET) $_2$ Cu $_2$ (CN) $_3$ and κ -(ET) $_2$ Cu $_2$ [N(CN) $_2$]Cl. Both measurements were performed in the ambient pressure Mott insulating phases of the two compounds. In κ -(ET) $_2$ Cu $_2$ [N(CN) $_2$]Cl a rapid upturn in the susceptibility is observed at ~ 25 K as a result of the Néel transition. Remarkably no magnetic ordering transition is observed in κ -(ET) $_2$ Cu $_2$ (CN) $_3$ down to the lowest temperatures studied (32 mK). Fits of series expansion data (lines in figure) to the measured susceptibility [165] show that the exchange interaction, J , is about 250 K in both materials. This had led to the suggestion that it is the greater frustration in κ -(ET) $_2$ Cu $_2$ (CN) $_3$ that leads to a spin-liquid ground state. [In κ -(ET) $_2$ Cu $_2$ (CN) $_3$ $J'/J \sim 1$ whereas in κ -(ET) $_2$ Cu $_2$ [N(CN) $_2$]Cl $J'/J < 1$.] The right panel shows similar measurements in β' -[Pd(dmit) $_2$] $_2$ Z [170]. This data is also well described by series expansions for the isotropic triangular lattice (solid lines in figure with J marked). Except for X =Et $_2$ Me $_2$ Sb the β' -[Pd(dmit) $_2$] $_2$ Z salts do eventually order magnetically, but this suggests that it may be possible to use chemistry and/or uniaxial stress tune the β' -[Pd(dmit) $_2$] $_2$ Z salts across the antiferromagnetic/spin-liquid phase boundary. Understanding the microscopic nature of these spin-liquid states and why they are stabilised over the 120° -state which appears to be the ground state of Heisenberg model on the isotropic triangular lattice present major challenges to theory.

Et $_2$ Me $_2$ Y, Y=P or Sb, Me=CH $_3$ and Et=C $_2$ H $_5$. So far, this has not attracted so much attention from theorists as the κ -(ET) $_2$ Cu $_2$ (CN) $_3$ results, but these materials are also excellent candidates for the observation of spin-liquid states. The susceptibility of the β' -[Pd(dmit) $_2$] $_2$ Z compounds is much more reminiscent of that of κ -(ET) $_2$ Cu $_2$ (CN) $_3$ than that of κ -(ET) $_2$ Cu $_2$ [N(CN) $_2$]Cl. In particular the Et $_2$ Me $_2$ Sb salt shows no indications of magnetic ordering down to 4.3 K (the lowest temperature studied thus far, although magnetic impurities cause a Curie tail and make this somewhat difficult to substantiate) [197].

Further, the range of Curie temperatures seen in the salts that do eventually order magnetically [197] suggests that varying the cation, Z , in the β' -[Pd-(dmit)₂]₂ Z series allows one to tune the frustration and thus the proximity to the spin-liquid state.

The clear theoretical challenge is to explain why a spin-liquid ground state is stable in these materials.¹³ Simply appealing to the geometrical frustration inherent in the triangular lattice is insufficient, as it is all but certain that the 120°-state is the ground state of Heisenberg model on a triangular lattice (see section 1.7). A great deal of theoretical effort has already been expended on this problem [30, 56, 145, 149, 161, 188–195]. The idea that proximity to the Mott transition allows perturbation terms not included in the Heisenberg model to become large seems particularly promising. However, this question is far from settled yet and will doubtless be the basis of much debate in the future.

1.9 Conclusions

We have seen above that the predicted behaviour of the Hubbard model on the anisotropic triangular lattice provides good qualitative agreement with experiments on the organic charge transfer salts. This success is not just limited to the κ phases but the model applies equally well to the β , β' and λ phases: in spite of the chemical and structural differences between these materials the physics is essentially the same. As the exact solution of this model is not yet known various approximation schemes must be used to discover the true behaviour of the model. Perhaps the most notable successes of this model are the explanation of the metallic state and the Mott transition in terms of dynamical mean field theory (DMFT) discussed in section 1.3.1. However, recent theories of superconductivity based on the resonating valence bond (RVB) state appear to explain many of the features of the superconducting state. An important test of the RVB theory will be a detailed comparison of its prediction of a pseudogap with experiments (such as NMR or Nernst effect) on the strongly correlated metallic state just above T_c . An important challenge for this theory is to explain the small superfluid stiffness seen far from the Mott transition, i.e., in compounds with low critical temperatures.

There are many exciting challenges facing the field. Some are old - like finding an experiment which decisively settles the questions about the pairing symmetry; while others are extremely new - like understanding the spin-liquid state in κ -(ET)₂Cu₂(CN)₃. An important challenge is also to increase the quantitative detail of the predictions of theory. This is required, not only because of intrinsic interest in the organic charge transfer salts themselves, but also because the organic charge transfer salts provide a wonderful test-bed

¹³Even if the compounds do order at some extremely low temperature the spin-liquid state is clearly at least very energetically competitive.

for many of the most important ideas in the theory of strongly correlated materials. In particular, the Mott transition remains perhaps *the* phenomena of central importance to strongly correlated physics and the organic charge transfer salts are one of only a handful of systems where the Mott transition can be driven by varying U/W as Mott originally envisioned [198] rather than by doping. We have highlighted one possible approach to increasingly quantitative prediction, that of parameterising minimal models, although there are several other approaches which might be profitable, such as LDA+DMFT [199].

We hope that this review has made it clear that the organic charge transfer salts are a playground for quantum many-body physics.¹⁴ Many of the most important phenomena in strongly correlated physics are found in the organic charge transfer salts, for example, the Mott transition, unconventional superconductivity, frustrated antiferromagnetism and spin-liquids. Further, the organic charge transfer salts are exceptionally clean systems (as is evidenced by the beautiful quantum oscillations observed at low temperatures [40,41,171]). But, perhaps, what makes the organic charge transfer salts most attractive is the relative ease with which the strength of correlations can be controlled via hydrostatic pressure or chemistry [8,28]. Thus, the study of the organic charge transfer salts is an important branch of strongly correlated physics. The lessons learned from the organic charge transfer salts are already having significant impact in other strongly correlated systems. For example, the spin-liquid phase of Cs_2CuCl_4 has a great deal in common with the insulating phases of $\kappa\text{-(ET)}_2\text{Cu}_2(\text{CN})_3$ and $\beta'\text{-[Pd(dmit)}_2\text{)]}_2\text{Z}$ [56] and the ‘Curie-Weiss metal’ seen in Na_xCoO_2 is essentially a doped analogue of the ‘bad metal’ observed in the organic charge transfer salts [11]. All of these phenomena arise from the interplay of strong correlations with frustration which can be so elegantly studied in the organic charge transfer salts.

Acknowledgements

We are indebted to many people for useful discussions and collaborations without which this review would not be possible. In particular we would like to thank James Analytis, Arzhang Ardavan, Steve Blundell, Jim Brooks, Tony Carrington, Amalia Coldea, Martin Dressel, John Fjærestad, Greg Freebairn, Hidetoshi Fukuyama, Anthony Jacko, Michael Lang, Fumitaka Kagawa, Kazushi Kanoda, Brad Marston, Jaime Merino, Mark Pederson, Francis Pratt, Edan Scriven, John Singleton, Hiromi Taniguchi, Jochen Wosnitza and Eddy Yusuf. We are grateful to Edan Scriven and Eddy Yusuf for critically reading this manuscript. We are also indebted to the Australian Research Council for funding our work over a number of years.

¹⁴Although it has suggested that the organic charge transfer salts are a “minefield” rather than a playground [200]!

References

1. See, for example, table 1. 1 in N. Ashcroft and D. Mermin, *Solid State Physics* (Thomson Learning, Singapore, 1976).
2. L. D. Landau, Sov. Phys. JETP **3**, 920 (1957).
3. A. C. Hewson, *The Kondo Problem to Heavy Fermions* (Cambridge University Press, Cambridge, 1997).
4. J. Bardeen, L. N. Cooper, and J. R. Schrieffer, Phys. Rev. **108**, 1175 (1957).
5. P. A. Lee, N. Nagaosa, and X.-G. Wen, Rev. Mod. Phys. **78**, 17 (2006).
6. M. B. Salamon and M. Jaime, Rev. Mod. Phys. **73**, 583 (2001).
7. For a review see M. Sigrist and K. Ueda, Rev. Mod. Phys. **63**, 239 (1991).
8. H. Taniguchi, K. Kanoda, and A. Kawamoto, Phys. Rev. B **67**, 014510 (2003).
9. T. Sasaki, N. Yoneyama, A. Suzuki, N. Kobayashi, Y. Ikemoto, and H. Kimura, J. Phys. Soc. Japan **74**, 2351 (2005).
10. P. W. Anderson, Science **235**, 1196 (1987).
11. For a recent review see J. Merino, B. J. Powell, and R. H. McKenzie, cond-mat/0512696 (to appear in Phys. Rev. B).
12. See, for example, A. Girlando, M. Masino, A. Brillante, R. G. DellaValle and E. Venuti, Phys. Rev. B **66**, 100507 (2002); G. Varelogiannis, Phys. Rev. Lett. **88**, 117005 (2002).
13. H. Elsinger, J. Wosnitza, S. Wanka, J. Hagel, D. Schweitzer, and W. Strunz, Phys. Rev. Lett. **84**, 6098 (2000); J. Müller, M. Lang, R. Helfrich, F. Steglich, and T. Sasaki, Phys. Rev. B **65**, 140509 (2002).
14. C. Strack, C. Akinci, V. Pashchenko, B. Wolf, E. Uhrig, W. Assmus, M. Lang, J. Schreuer, L. Wiehl, J. A. Schlueter, J. Wosnitza, D. Schweitzer, J. Müller, and J. Wykhoff, Phys. Rev. B **72**, 54511 (2005).
15. See, for example, M. Lang and J. Müller, *Organic superconductors in The Physics of Superconductors - Vol. 2*, K.-H. Bennemann, J. B. Ketterson (Eds.), Springer-Verlag (2003); T. Ishiguro, K. Yamaji, and G. Saito, *Organic Superconductors* (Springer Verlag, Heidelberg, 1998).
16. A. Fortunelli and A. Painelli, Phys. Rev. B **45**, 16088 (1997); J. Chem. Phys. **106**, 8041 (1997); **106**, 8051 (1997); S. A. French and C. R. A. Catlow, J. Phys. Chem. Solids **65**, 39 (2004).
17. Y. J. Lee, R. M. Nieminen, P. Ordejon, and E. Canadell, Phys. Rev. B **67**, R180505 (2003).
18. T. Miyazaki and H. Kino, Phys. Rev. B **68**, R220511 (2003).
19. T. Miyazaki and H. Kino, Phys. Rev. B **73**, 035107 (2006).
20. H. Kino and T. Miyazaki, cond-mat/0601063.
21. H. Kino and H. Fukuyama, J. Phys. Soc. Jpn. **65**, 2158 (1996).
22. J. Merino and R. H. McKenzie, Phys. Rev. Lett. **87**, 237002 (2001); R. H. McKenzie, J. Merino, J. B. Marston, and O. P. Sushkov, Phys. Rev. B **64**, 085109 (2001); A. Greco, J. Merino, A. Foussats, and R. H. McKenzie, Phys. Rev. B **71**, 144502 (2005).
23. H. Seo, J. Merino, H. Yoshioka, and M. Ogata, J. Phys. Soc. Japan **75**, 051009 (2006).
24. B. J. Powell, cond-mat/0603057.
25. R. H. McKenzie, Comments Condens. Matter Phys. **18**, 309 (1998).
26. M. Rahal, D. Chasseau, J. Gaultier, L. Ducasse, M. Kurmoo, and P. Day, Acta Cryst. B **53**, 159 (1997).

27. See for example, F. Castet, A. Fritsch, and L. Ducasse, *J. Phys. I* **6**, 583 (1996); L. Ducasse, A. Fritsch, and F. Castet, *Synth. Met.* **85**, 1627 (1997); A. Fortunelli and A. Painelli, *J. Chem. Phys.* **106**, 8051 (1997); Y. Imamura, S. Ten-no, K. Yonemitsu, and Y. Tanimura, *J. Chem. Phys.* **111**, 5986 (1999).
28. K. Kanoda, *Physica C* **282-287**, 299 (1997).
29. G. Freebairn, “*Phonons and the Isotopically Induced Mott Transition*”, Honours thesis, University of Queensland (2005).
30. B. J. Powell and R. H. McKenzie, *Phys. Rev. Lett.* **94**, 047004 (2005).
31. S. Uji, H. Shinagawa, T. Terashima, T. Yakabe, Y. Terai, M. Tokumoto, A. Kobayashi, H. Tanaka, and H. Kobayashi, *Nature* **410**, 908 (2001).
32. V. Jaccarino and M. Peter, *Phys. Rev. Lett.* **9**, 290 (1962). L. Balicas, J. S. Brooks, K. Storr, S. Uji, M. Tokumoto, H. Tanaka, H. Kobayashi, A. Kobayashi, V. Barzykin, and L. P. Gorkov, *Phys. Rev. Lett.* **87**, 067002 (2001).
33. O. Cépas, R. H. McKenzie, and J. Merino, *Phys. Rev. B* **65**, 100502(R) (2002).
34. S. Uji and J. S. Brooks, *J. Phys. Soc. Japan* **75**, 051014 (2006).
35. H. Kino and T. Miyazaki, *cond-mat/0601063*.
36. P. M. Grant, *Phys. Rev. B* **26**, 6888 (1982).
37. N. Dupuis, C. Bourbonnais, and J. C. Nickel, *cond-mat/0510544*.
38. G. Kotliar and D. Vollhardt, *Phys. Today* **57**, 53 (2004).
39. G. Kotliar and D. Vollhardt, *Phys. Today* **57**, 53 (2004); A. Georges, G. Kotliar, W. Krauth, and M. Rozenberg, *Rev. of Mod. Phys.* **68**, 125 (1996).
40. For a comprehensive review see J. Wosnitza, *Fermi Surfaces of Low-Dimensional Organic Metals and Superconductors: Springer Tracts in Modern Physics* **134** (Springer Verlag, Berlin, 1996).
41. For recent reviews see J. Singleton, *Rep. Prog. Phys.* **63** 1111 (2000); M. Kartsovnik, *Chem. Rev.* **104**, 5737 (2004).
42. L. N. Bulaevskii, *Adv. Phys.* **37**, 443 (1988).
43. J. G. Analytis, A. Ardavan, S. J. Blundell, R. L. Owen, E. F. Garman, C. Jeynes, and B. J. Powell, *Phys. Rev. Lett.* **96**, 177002 (2006).
44. See, for example, A. A. Abrikosov, *Introduction to the theory of normal metals* (Academic Press, New York, 1972).
45. W. Baber, *Proc. Roy. Soc. A* **158**, 383 (1937).
46. N. F. Mott, *Metal insulator transitions* (Taylor and Francis, London, 1990).
47. O. Gunnarsson, *Alkali-doped fullerenes: Narrow-band solids with unusual properties* (World Scientific, Singapore, 2004).
48. A. W. Tyler, A. P. Mackenzie, S. Nishizaki, and Y. Maeno, *Phys. Rev. B* **58**, R10107 (1998).
49. L. Klein, *Phys. Rev. Lett.* **77**, 2774 (1996); P. B. Allen, H. Berger, O. Chauvet, L. Forro, T. Jarlborg, A. Junod, B. Revaz, and G. Santi, *Phys. Rev. B* **53**, 4393 (1996).
50. P. B. Allen, R. M. Wentzcovitch, W. W. Schulz, and P. C. Canfield, *Phys. Rev. B* **48**, 4359 (1993).
51. K. Kornelsen, J. E. Eldridge, C. C. Homes, H. H. Wang, and J. M. Williams, *Solid State Commun.* **72**, 475 (1989); J. E. Eldridge, K. Kornelsen, H. H. Wang, J. M. Williams, A. V. S. Crouch, and D. M. Watkins, *Solid State Commun.* **79**, 583 (1991); M. Tamura, H. Tajima, K. Yakushi, H. Kuroda, A. Kobayashi, R. Kato, and H. Kobayashi, *J. Phys. Soc. Jpn.* **60**, 3861 (1991); M. Dressel, J. E. Eldridge, H. H. Wang, U. Geiser, and J. M. Williams, *Synth. Met.* **52**, 201 (1992); C. S. Jacobsen, J. M. Williams, and H. H. Wang, *Solid State Commun.*

- 54, 937 (1985); C. S. Jacobsen, D. B. Tanner, J. M. Williams, U. Geiser, and H. H. Wang, Phys. Rev. B **35**, 9605 (1987); J. Dong, J. L. Musfeldt, J. A. Schlueter, J. M. Williams, P. G. Nixon, R. W. Winter, and G. L. Gard, Phys. Rev. B **60**, 4342 (1999); A. Schwartz, M. Dressel, G. Gruner, V. Vescoli, L. Degiorgi, and T. Giamarchi, Phys. Rev. B **58**, 1261 (1998).
52. P. Limelette, P. Wzietek, S. Florens, A. Georges, T. A. Costi, C. Pasquier, D. Jérôme, C. Mézière, and P. Batail, Phys. Rev. Lett. **91**, 016401 (2003).
53. R. C. Yu, J. M. Williams, H. H. Wang, J. E. Thompson, A. M. Kini, K. D. Carlson, J. Ren, M.-H. Whangbo, and P. M. Chaikin, Phys. Rev. B **44**, 6932 (1991).
54. J. Merino and R. H. McKenzie, Phys. Rev. B **61**, 7996 (2000).
55. A. P. Ramirez, Annu. Rev. Mater. Sci. **24**, 453 (1994); P. Schiffer and I. Daruka, Phys. Rev. B **56**, 13712 (1997).
56. W. Zheng, R. R. P. Singh, R. H. McKenzie, and R. Coldea, Phys. Rev. B **71**, 134422 (2005).
57. B. Andraka, J. S. Kim, G. R. Stewart, K. D. Carlson, H. H. Wang, and J. M. Williams, Phys. Rev. B **40**, 11345 (1989); B. Andraka, C. S. Jee, J. S. Kim, G. R. Stewart, K. D. Carlson, H. H. Wang, A. V. S. Crouch, A. M. Kini, and J. M. Williams, Solid State Comm. **79** 57 (1991).
58. R. C. Haddon, A. P. Ramirez, and S. H. Glarum, Adv. Mater. **6**, 316 (1994).
59. K. Frikach, M. Poirier, M. Castonguay, and K. D. Truong, Phys. Rev. B **61**, R6491 (2000).
60. D. Fournier, M. Poirier, M. Castonguay, and K. D. Truong, Phys. Rev. Lett. **90**, 127002 (2003).
61. J. Merino and R. H. McKenzie, Phys. Rev. B **24**, 16442 (2000).
62. S. R. Hassan, A. Georges, and H. R. Krishnamurthy, Phys. Rev. Lett. **94**, 036402 (2005).
63. R. H. McKenzie, cond-mat/9905044.
64. N. E. Hussey, J. Phys. Soc. Japan **74**, 1107 (2005).
65. A. Jacko, private communication (2006).
66. M. Weger, J. Low Temp. Phys. **95**, 131 (1994); M. Weger and D. Schweitzer, Synth. Met. **70**, 889 (1995); J. Hagel, J. Wosnitza, C. Pfleiderer, J. A. Schlueter, J. Mohtasham, and G. L. Gard, Phys. Rev. B **68**, 104504 (2003).
67. R. Bulla, T. A. Costi, and D. Vollhardt, Phys. Rev. B **64**, 045103 (2001).
68. P. Limelette, A. Georges, D. Jerome, P. Wzietek, P. Metcalf, and J. M. Honig, Science **302**, 89 (2003).
69. N. Goldenfeld, *Lectures on Phase Transitions and the Renormalization Group* (Westview, Boulder, 1992).
70. F. Kagawa, K. Miyagawa, and K. Kanoda, Nature **534**, 89 (2005).
71. M. Imada, Phys. Rev. B **72**, 075113 (2005); J. Phys. Soc. Jpn. **74**, 859 (2005).
72. T. Misawa, Y. Yamaji, and M. Imada, cond-mat/0604387.
73. T. E. Weller, M. Ellerby, S. S. Saxena, R. P. Smith, and N. T. Skipper, Nature Phys. **1**, 39 (2005).
74. A. P. Micolich, E. Tavener, B. J. Powell, A. R. Hamilton, M. Curry, R. Geidd, and P. Meredith, cond-mat/0509278.
75. G. M. Eliashberg, JETP **38**, 966 (1960); JETP **39**, 1437 (1960).
76. M. Lüders, M. A. L. Marques, N. N. Lathiotakis, A. Floris, G. Profeta, L. Fast, A. Continenza, S. Massidda, and E. K. U. Gross, Phys. Rev. B **72**, 024545 (2005); M. A. L. Marques, M. Lüders, N. N. Lathiotakis, G. Profeta, A. Floris, L. Fast, A. Continenza, E. K. U. Gross, and S. Massidda, Phys. Rev. B **72**, 024546 (2005).

77. See, for example, J.B. Ketterson and S.N. Song, *Superconductivity* (Cambridge University Press, Cambridge, 1999).
78. J. F. Annett, *Adv. Phys.* **39**, 83 (1990).
79. See, for example, M. Tinkham, *Group Theory and Quantum Mechanics* (McGraw-Hill, New York, 1964).
80. R. W. Morse, T. Olsen, and J. D. Gavenda, *Phys. Rev. Lett.* **3**, 15 (1959).
81. A. J. Leggett, *Rev. Mod. Phys.* **37**, 331 (1975).
82. D. Vollhardt and P. Wölfle, *The Superfluid Phases of Helium 3* (Taylor and Francis, London, 1990).
83. S. M. deSoto, C. P. Slichter, A. M. Kini, H. H. Wang, U. Geiser, and J. M. Williams, *Phys. Rev. B* **52**, 10364 (1995).
84. H. Mayaffre, P. Wzietek, D. Jérôme, C. Lenoir, and P. Batail, *Phys. Rev. Lett.* **75**, 4122 (1995).
85. K. Miyagawa, K. Kanoda, and A. Kawamoto, *Chem. Rev.* **104**, 5635 (2004).
86. R. Balian and N. R. Werthamer, *Phys. Rev.* **131**, 1553 (1963).
87. F. Zuo, J. S. Brooks, R. H. McKenzie, J. A. Schlueter, and J. M. Williams, *Phys. Rev. B* **61**, 750 (2000).
88. A. M. Clogston, *Phys. Rev. Lett.* **9**, 266 (1962).
89. B. S. Chandrasekhar, *Appl. Phys. Lett.* **1**, 7 (1962).
90. B. J. Powell, J. F. Annett, and B. L. Györfly, *J. Phys. A* **36**, 9289 (2003); *J. Phys.: Condens. Matter* **15**, L235 (2003).
91. K. Murata, M. Tokumoto, H. Anzai, K. Kajimura, and T. Ishiguro, *J. Appl. Phys.* **26**, 1367 (1987).
92. M.-S. Nam, J. A. Symington, J. Singleton, S. J. Blundell, A. Ardavan, J. A. A. J. Perenboom, M. Kurmoo, and P. Day, *J. Phys.: Condens. Matter* **11**, 477 (1999).
93. K. Izawa, H. Yamaguchi, T. Sasaki, and Y. Matsuda, *Phys. Rev. Lett.* **88**, 27002 (2002).
94. B. J. Powell, cond-mat/0606188.
95. A. Carrington, I. J. Bonalde, R. Prozorov, R. W. Giannetta, A. M. Kini, J. Schlueter, H. H. Wang, U. Geiser, and J. M. Williams, *Phys. Rev. Lett.* **83**, 4172 (1999).
96. B. J. Powell and R. H. McKenzie, *Phys. Rev. B* **69**, 024519 (2004).
97. P. W. Anderson, *J. Phys. Chem. Solids* **11**, 26 (1959).
98. D. J. van Harlingen, *Rev. Mod. Phys.* **67**, 515 (1995).
99. K. M. Lang, V. Madhavan, J. E. Hoffman, E. W. Hudson, H. Elsakl, S. Uchida, and J. C. Davis, *Nature* **415**, 412 (2002); E. W. Hudson, K. M. Lang, V. Madhavan, S. H. Pan, H. Elsakl, S. Uchida, and J. C. Davis, *Nature* **411**, 920 (2001); S. H. Pan, E. W. Hudson, K. M. Lang, H. Elsakl, S. Uchida, and J. C. Davis, *Nature* **403**, 746 (2000).
100. See, for example, V.P. Mineev and K.V. Samokhin, *Introduction to Unconventional Superconductivity* (Gordon and Breach, Amsterdam, 1998).
101. A. Larkin, *JETP Lett.* **2**, 130 (1965).
102. A. A. Abrikosov and L. P. Gorkov, *Sov. Phys. JETP* **12**, 1243 (1961).
103. A. A. Abrikosov, *Rev. Mod. Phys.* **76**, 975 (2004).
104. See, for example, J. F. Annett, *Superconductivity, Superfluids and Condensates* (Oxford University Press, Oxford, 2004).
105. See, for example, F.L. Pratt, S.J. Blundell, T. Lancaster, M.L. Brooks, S.L. Lee, N. Toyota and T. Sasaki, *Synthetic Metals* **152**, 417 (2005) and references therein.

106. For a recent review see R. Joynt and L. Taillefer, *Rev. Mod. Phys.* **74**, 235 (2002).
107. For a recent review see A.P. Mackenzie and Y. Maeno, *Rev. Mod. Phys.* **75**, 657 (2003).
108. G.E. Volovik, *JETP Lett.* **58**, 469 (1993).
109. C. Kübert and P.J. Hirschfeld, *Solid State Commun.* **105**, 459 (1998).
110. I. Vekter, P. Hirschfeld, J. Carbotte, and E. Nicol, *Phys. Rev. B* **59**, R9023 (1999); I. Vekter, P.J. Hirschfeld, and E.J. Nicol, *Phys. Rev. B* **64**, 60513 (2001).
111. L. N. Bulaevskii, M. J. Graf, and M. P. Maley, *Phys. Rev. Lett.* **83**, 388 (1999).
112. K. Deguchi, Z. Mao, H. Yaguchi, and Y. Maeno, *Phys. Rev. Lett.* **92**, 47002 (2004).
113. H. Won and K. Maki, *Europhys. Lett.* **30**, 421 (1995).
114. S.H. Simon and P.A. Lee, *Phys. Rev. Lett.* **78**, 1548 (1997).
115. K. A. Moler, D. J. Baar, J. S. Urbach, R. Liang, W. N. Hardy, and A. Kapitulnik, *Phys. Rev. Lett.* **73**, 2744 (1994); R.A. Fisher, J.E. Gordon, S.F. Reklis, D.A. Wright, J.P. Emerson, B.F. Woodfield, E.M. McCarron III, and N.E. Phillips, *Physica C* **252**, 237 (1995); B. Revaz, J.-Y. Genoud, A. Junod, K. Neumaier, A. Erb, and E. Walker, *Phys. Rev. Lett.* **80**, 3364 (1998); D. A. Wright, J. P. Emerson, B. F. Woodfield, J. E. Gordon, R. A. Fisher, and N. E. Phillips, *Phys. Rev. Lett.* **82**, 1550 (1999).
116. R. Fisher, N. Phillips, A. Schilling, B. Buffeteau, R. Calemczuk, T. Hargreaves, C. Marcenat, K. Dennis, R. McCallum, and A. O'Connor, *Phys. Rev. B* **61**, 1473 (2000).
117. K. Maki, *Phys. Rev.* **158**, 397 (1967).
118. J. Lowell and J.B. Sousa, *J. Low Temp. Phys.* **3**, 65 (1970).
119. H. Aubin, K. Behnia, M. Ribault, R. Gagnon, and L. Taillefer, *Phys. Rev. Lett.* **78**, 2624 (1997).
120. J. Moreno and P. Coleman, *Phys. Rev. B* **53**, 2995 (1996).
121. H. Suderow, H. Aubin, K. Behnia, and A. Huxley, *Phys. Lett. A* **234**, 64 (1997).
122. M. A. Tanatar, S. Nagai, Z. Q. Mao, Y. Maeno, and T. Ishiguro, *Phys. Rev. B* **63**, 064505 (2001); M. A. Tanatar, M. Suzuki, S. Nagai, Z. Q. Mao, Y. Maeno, and T. Ishiguro, *Phys. Rev. Lett.* **86**, 2649 (2001); K. Izawa, H. Takahashi, H. Yamaguchi, Y. Matsuda, M. Suzuki, T. Sasaki, T. Fukase, Y. Yoshida, R. Settai, and Y. Onuki, *Phys. Rev. Lett.* **86**, 2653 (2001).
123. T. Dahm, H. Won, and K. Maki, cond-mat/0006301.
124. M. A. Tanatar, T. Ishiguro, H. Tanaka, and H. Kobayashi, *Phys. Rev. B* **66**, 134503 (2002); M.A. Tanatar, M. Suzuki, T. Ishiguro, H. Tanaka, H. Fujiwara, H. Kobayashi, T. Toito, and J. Yamada, *Synth. Met.* **137**, 1291 (2003); M.A. Tanatar, M. Suzuki, T. Ishiguro, H. Fujiwara, and H. Kobayashi, *Physica C* **388-389**, 613 (2003); M.A. Tanatar, T. Ishiguro, H. Tanaka, and H. Kobayashi, *Synth. Met.* **133-134**, 215 (2003).
125. M. Tinkham, *Introduction to Superconductivity* (McGraw-Hill, New York, 1975).
126. B. Ellman, L. Taillefer, and M. Poirier, *Phys. Rev. Lett.* **54**, 9043 (1996).
127. B. Shivaram, Y. Jeong, T. Rosenbaum, and D. Hinks, *Phys. Rev. Lett.* **56**, 1078 (1986).
128. C. Lupien, W. MacFarlane, C. Proust, L. Taillefer, Z. Mao, and Y. Maeno, *Phys. Rev. Lett.* **86**, 5986 (2001); H. Matsui, Y. Yoshida, A. Mukai, R. Settai,

- Y. Onuki, H. Takei, N. Kumura, H. Aoki, and N. Toyota, J. Phys. Soc. Jpn. **69**, 3769 (2000); H. Matsui, Y. Yoshida, A. Mukai, R. Settai, Y. Onuki, H. Takei, N. Kumura, H. Aoki, and N. Toyota, Phys. Rev. B **63**, R60505 (2001).
129. M. Yoshizawa, T. Kumada, and N. Yoshimoto, J. Low Temp. Phys. **105**, 1745 (1996).
130. T. Simizu, N. Yoshimoto, M. Nakamura, and M. Yoshizawa, Physica B **281&282**, 896 (2000).
131. K. Frikach, P. Fertey, M. Poirier, and K. Troung, Synth. Met. **103**, 2081 (1999).
132. Y. J. Uemura, G. M. Luke, B. J. Sternlieb, J. H. Brewer, J. F. Carolan, W. N. Hardy, R. Kadono, J. R. Kempton, R. F. Kiefl, S. R. Kreitzman, P. Mulhern, T. M. Riseman, D. L. Williams, B. X. Yang, S. Uchida, H. Takagi, J. Gopalakrishnan, A. W. Sleight, M. A. Subramanian, C. L. Chien, M. Z. Cieplak, G. Xiao, V. Y. Lee, B. W. Statt, C. E. Stronach, W. J. Kossler, and X. H. Yu, Phys. Rev. Lett. **62**, 2317 (1989).
133. V. J. Emery and S. A. Kivelson, Nature **374**, 434 (1995).
134. F. C. Zhang, C. Gross, T. M. Rice, and H. Shiba, Supercond. Sci. Technol. **1**, 36 (1988).
135. Z. Szotek, B. L. Györfy, and W. M. Temmerman, Phys. Rev. B **62**, 3997 (2000).
136. H. Mook, Phys. Rev. Lett. **32**, 1167 (1974).
137. For a recent review see, for example, §4 of A. Griffin, *Excitations in a Bose-Condensed Liquid* (Cambridge University Press, Cambridge, 1993).
138. F. L. Pratt, S. J. Blundell, I. M. Marshall, T. Lancaster, S. L. Lee, A. Drew, U. Divakar, H. Matsui, and N. Toyota, Polyhedron **22**, 2307 (2003).
139. M. Lang, N. Toyota, T. Sasaki, and H. Sato, Phys. Rev. B **46**, 5822 (1992).
140. M. I. Larkin, A. Kinkhabwala, Y. J. Uemura, Y. Sushko, and G. Saito, Phys. Rev. B **64**, 144514 (2001).
141. B. J. Powell and R. H. McKenzie, J. Phys.: Condens. Matter **16**, L367 (2004).
142. F. L. Pratt and S. J. Blundell, Phys. Rev. Lett. **94**, 097006 (2005).
143. K. Kuroki, J. Phys. Soc. Japan, **75**, 051013 (2006).
144. B. J. Powell and R. H. McKenzie, cond-mat/0607079.
145. J. Liu, J. Schmalian, and N. Trivedi, Phys. Rev. Lett. **94**, 127003 (2005).
146. J. Y. Gan, Y. Chen, Z. B. Su, and F. C. Zhang, Phys. Rev. Lett. **94**, 067005 (2005).
147. S. Yunoki and S. Sorella, cond-mat/0602180.
148. P. Sahebsara and D. Sénéchal, cond-mat/0604057.
149. B. Kyung and A.-M. S. Tremblay, cond-mat/0604377.
150. R. Laughlin, cond-mat/0209269.
151. J. Gan, F. C. Zhang, and Z. B. Su, Phys. Rev. B **71**, 014508 (2005).
152. W. F. Brinkman and T. M. Rice, Phys. Rev. B **2**, 4302 (1970).
153. E. H. Lieb and F. Y. Wu, Phys. Rev. Lett. **20**, 1445 (1968).
154. K. Aryanpour, W. E. Pickett, and R. T. Scalettar, cond-mat/0604609.
155. M. Capone, L. Capriotti, F. Becca, and S. Caprara, Phys. Rev. B **63**, 085104 (2001).
156. Z. Weihong, R. H. McKenzie, and R. R. P. Singh, Phys. Rev. B **59**, 14367 (1999).
157. J. Merino, R. H. McKenzie, J. B. Marston, and C. H. Chung, J. Phys.: Condens. Matter **11**, 2965 (1999).
158. C. H. Chung, J. B. Marston, and R. H. McKenzie, J. Phys.: Condens. Matter **13**, 5159 (2001).

159. A. Chubukov, S. Sachdev, and T. Senthil, *J. Phys.: Condens. Matter* **6**, 8891 (1994).
160. B. Bernu, P. Lecheminant, C. Lhuillier, and L. Pierre, *Phys. Rev. B* **50**, 10048 (1994); L. Capriotti, A. E. Trumper, and S. Sorella *Phys. Rev. Lett.* **82**, 3899 (1999); D. Huse and V. Elser, *Phys. Rev. Lett.* **60**, 2531 (1988); D. J. J. Farnell, R. F. Bishop, and K. A. Gernoth, *Phys. Rev. B* **63**, 220402 (2001); R. R. P. Singh and D. A. Huse, *Phys. Rev. Lett.* **68**, 1766 (1992).
161. O. I. Motrunich, *Phys. Rev. B* **72**, 045105 (2005).
162. R. H. McKenzie, *Science* **278**, 820 (1997).
163. R. Coldea, D. A. Tennant, K. Habicht, P. Smeibidl, C. Wolters, and Z. Tylczynski, *Phys. Rev. Lett.* **88**, 137203 (2002).
164. R. Coldea, D. A. Tennant, A. M. Tsvelik, and Z. Tylczynski, *Phys. Rev. Lett.* **86**, 1335 (2001).
165. Y. Shimizu, K. Miyagawa, K. Kanoda, M. Maesato, and G. Saito, *Phys. Rev. Lett.* **91**, 107001 (2003).
166. H. Kobayashi, R. Kato, and A. Kobayashi, *synth. Met.* **19**, 263 (1987); T. Mori and H. Sasaki, *Solid State Commun.* **62**, 525 (1987).
167. S.-W. Tsai and J. B. Marston, *Can. J. Phys.* **79**, 1463 (2001).
168. See, for example, A. M. Tsvelik, *Quantum Field Theory in Condensed Matter Physics* (Cambridge Univ. Press, Cambridge, 2003).
169. M. Bocquet, F. H. L. Essler, A. M. Tsvelik, and A. O. Gogolin, *Phys. Rev. B* **64**, 094425 (2001); O. A. Starykh and L. Balents *Phys. Rev. Lett.* **93**, 127202 (2004).
170. M. Tamura and R. Kato, *J. Phys.: Condens. Matter* **14**, L729 (2002).
171. N. Harrison, E. Rzepniewski, J. Singleton, P. J. Gee, M. M. Honold, P. Day, and M. Kurmoo, *J. Phys.: Condens. Matter* **11**, 7227 (1999); J. Caulfield, W. Lubczynski, F. L. Pratt, J. Singleton, D. Y. K. Ko, W. Hayes, M. Kurmoo and P. Day, *J. Phys.: Condens. Matter* **6** 2911 (1994).
172. S. Goedecker, *Rev. Mod. Phys.* **71**, 1085 (1999).
173. M. R. Pederson and A. A. Quong, *Phys. Rev. B* **46**, 13584 (1992); V. P. Antropov, O. Gunnarsson, and F. Reuse, *Phys. Rev. B* **46**, 13647 (1992).
174. E. W. Carlson, V. J. Emery, S. A. Kivelson, and D. Orgad, in *The Physics of Superconductors - Vol. 2*, edited by K.-H. Bennemann and J. B. Ketterson (Springer Verlag, Berlin, 2003).
175. P. Wzietek, H. Mayaffre, D. Jérôme, and S. Brazovskii, *J. Phys. I* **6**, 2011 (1996).
176. T. Maier, M. Jarrell, T. Pruschke, and M. H. Hettler, *Rev. Mod. Phys.* **77**, 1027 (2005).
177. E.C. Carter and A. J. Scholfield, *Phys. Rev. B* **70**, 045107 (2004); S. S. Kancharla, M. Civelli, M. Capone, B. Kyung, D. Senechal, G. Kotliar, A.-M.S. Tremblay, cond-mat/0508205.
178. For a recent review see Y. Wang, L. Li, and N. P. Ong, cond-mat/0510470.
179. A. Millis, H. Monien, and D. Pines, *Phys. Rev. B* **42**, 1671 (1990).
180. T. Moriya and K. Ueda, *Adv. Phys.* **49**, 555 (2000).
181. E. Yusuf, private communication (2006).
182. J. M. Harris, Z.-X. Shen, P. J. White, D. S. Marshall, M. C. Schabel, J. N. Eckstein, and I. Bozovic, *Phys. Rev. B* **54**, R15665 (1996). H. Ding, T. Yokoya, J. C. Campuzano, T. Takahashi, M. Randeria, M. R. Norman, and T. M. K. H. J. Giapintzakis, *Nature* **382**, 51 (1996).

183. A. Kanigel, M. R. Norman, M. Randeria, U. Chatterjee, S. Suoma, A. Kaminski, H. M. Fretwell, S. Rosenkranz, M. Shi, T. Sato, T. Takahashi, Z. Z. Li, H. Raffy, K. Kadowaki, D. Hinks, L. Ozyuzer, and J. C. Campuzano, *cond-mat/0605499*.
184. D. Basov, H. A. Mook, B. Dabrowski, and T. Timusk, *Phys. Rev. B* **52**, R13141 (1995); M. Arai, T. Nishijima, Y. Endoh, T. Egami, S. Tajima, K. Tomimoto, Y. Shiohara, M. Takahashi, A. Garrett, and S. M. Bennington, *Phys. Rev. Lett.* **83**, 608 (1999).
185. A. Boothroyd, R. Coldea, D. A. Tennant, D. Prabhakaran, L. Helme, and C. D. Frost, *Phys. Rev. Lett.* **92**, 197201 (2004); S. P. Bayrakci, I. Mirebeau, P. Bourges, Y. Sidis, M. Enderle, J. Mesot, D. P. Chen, C. T. Lin, and B. Keimer, *Phys. Rev. Lett.* **94**, 157205 (2005); L. M. Helme, A. T. Boothroyd, R. Coldea, D. Prabhakaran, D. A. Tennant, A. Hiess, and J. Kulda, *Phys. Rev. Lett.* **94**, 157206 (2005).
186. H. Taniguchi, R. Sato, K. Satoh, A. Kawamoto, H. Okamoto, T. Kobayashi, and K. Mizuno, to appear in the proceedings of the Sixth International Symposium on Crystalline Organic Metals, Superconductors, and Ferromagnets (ISCOM) September 11-16, 2005, Key West, Florida.
187. Y. Shimizu, K. Miyagawa, K. Kanoda, M. Maesato, and G. Saito, *Prog. Theo. Phys. Sup.* **159**, 52 (2005).
188. W. Zheng, J. O. Fjærestad, R. R. P. Singh, R. H. McKenzie, and R. Coldea, *Phys. Rev. Lett.* **96**, 057201 (2006).
189. J. Alicea, O. I. Motrunich, M. Hermele, and M. P. A. Fisher, *Phys. Rev. B* **72**, 064407 (2005).
190. K. S. Raman, R. Moessner, and S. L. Sondhi, *Phys. Rev. B* **72**, 064413 (2005).
191. P. Nikolić, *Phys. Rev. B* **72**, 064423 (2005).
192. S.-S. Lee and P. A. Lee, *Phys. Rev. Lett.* **95**, 036403 (2005).
193. A. Singh, *Phys. Rev. B* **71**, 214406 (2005).
194. O. Parcollet, G. Biroli, and G. Kotliar, *Phys. Rev. Lett.* **92**, 226402 (2004).
195. H. Kondo and T. Moriya, *J. Phys. Soc. Japan* **73**, 812 (2004).
196. T. Komatsu, N. Matsukawa, T. Inoue, and G. Saito, *J. Phys. Soc. Japan* **65**, 1340 (1996).
197. T. Nakamura, T. Takahashi, S. Aonuma, and R. Kato, *J. Mater. Chem.* **11**, 2159 (2001).
198. N. F. Mott, *Proc. Phys. Soc., London, Sect. A* **62**, 416 (1949).
199. C. A. Marianetti, G. Kotliar, and G. Ceder, *Nature Materials* **3**, 627 (2004).
200. P. W. Anderson, private communication (2001).